journal of the mechanical behavior of biomedical materials 160 (2024) 106782

Contents lists available at ScienceDirect

Journal of the Mechanical Behavior of Biomedical Materials

journal homepage: www.elsevier.com/locate/jmbbm

A comprehensive systematic review of marketed bone grafts for load-bearing critical-sized bone defects

Davide Ninarello [a,*], Alberto Ballardini [b], Giacomo Morozzi [b], Luigi La Barbera [a,c]

[a] Laboratory of Biological Structure Mechanics, Department of Chemistry, Materials and Chemical Engineering "Giulio Natta", Politecnico di Milano, Milan, Italy
[b] Greenbone Ortho S.p.A., Faenza, Italy
[c] IRCCS Galeazzi-Sant'Ambrogio Hospital, Milan, Italy

ARTICLE INFO

Keywords:
Bone grafts
Scaffold
Load-bearing district
Morphology
Mechanical properties

ABSTRACT

Treatment of critical-sized bone defects typically involves implantation of a bone graft. Various types of bone grafts are nowadays marketed, categorized by their origin as allografts, xenografts, or synthetic grafts. Despite their widespread use, a comprehensive understanding of their morphology and mechanical response remains elusive. Controlling these characteristics for promoting bone growth and ensuring mechanical resistance remains challenging, especially in load-bearing districts. This study aims to systematically review existing literature to delineate the principal morpho-mechanical characteristics of marketed bone grafts designed for load-bearing applications. Furthermore, the obtained data are organized and deeply discussed to find out the relationship between different graft characteristics. Among 196 documents identified through PRISMA guidelines, encompassing scientific papers and 510(k) documents, it was observed that a majority of marketed bone grafts exhibited porosity akin to bone (>60%) and mechanical properties resembling those of low-bone volume fraction trabecular bone. The present review underscores the dearth of information regarding the morpho-mechanical characteristics of bone grafts and the incomparability of data derived from different studies, due to the absence of suitable standards and guidelines. The need for new standards and complete and transparent morpho-mechanical characterization of marketed bone grafts is finally emphasized. Such an approach would enhance the comparability of data, aiding surgeons in selecting the optimal device to meet patient's needs.

1. Introduction

The choice of suitable treatment for large bone defects remains controversial. There is no unique definition of critical-sized defect (CSD); however, it is typically considered a defect that cannot heal spontaneously. CSDs can be generated by high-energy trauma, tumour resection, blast injuries, etc. (Nauth et al., 2018), and principal treatments consist of autografts, allografts, xenografts (XGs) or synthetic grafts (SGs). Autografts are considered the gold standard for treating CSDs due to their main advantages: osteogenesis, osteoinduction, osteoconduction, and histocompatibility (Chiarello et al., 2013). Osteogenesis is the ability to form new bone through osteogenic precursors, while osteoinduction and osteoconduction are respectively the graft capacity to induce the differentiation of mesenchymal cells into bone-forming and the ability to provide a structural morphology easily colonized by cells. The iliac crest is the primary source from which vascularized bone grafts are typically obtained. However, this approach leads to patient morbidity and longer surgical procedures, along with potential patient site infections and limited available bone volume (Schmidt, 2021). Alternatively, allografts and xenografts are widely used thanks to their properties similar to autografts with the advantage of having an almost unlimited available volume. Despite this, both present potential immunologic responses and the risk of transmitting diseases.

In this scenario, synthetic grafts are gaining interest based on the fact that they are indefinitely available, easily sterilized, avoiding any human pathogen contagion, controllable in both geometry and mechanical properties, and the surgical procedure is shortened thanks to the absence of graft harvesting (JBI Library of Systematic Reviews, 2010). The main issue regarding SGs is the selection of the material.

* Corresponding author. Laboratory of Biological Structure Mechanics, Department of Chemistry, Materials and Chemical Engineering "Giulio Natta", Politecnico di Milano, Piazza Leonardo da Vinci 32, 20133, Milan, Italy.
E-mail addresses: davide.ninarello@polimi.it (D. Ninarello), alberto.ballardini@greenbone.it (A. Ballardini), giacomo.morozzi@greenbone.it (G. Morozzi), luigi.labarbera@polimi.it (L. La Barbera).

https://doi.org/10.1016/j.jmbbm.2024.106782
Received 16 May 2024; Received in revised form 4 October 2024; Accepted 14 October 2024
Available online 18 October 2024

Several materials have been used both individually and as composites to merge the main properties of each. In particular, bioceramics are the most promising due to their similarity to the inorganic component of bone, together with the absence of dangerous ion release, high biocompatibility, strong scaffold-bone interfacial bonding, and bioactive behaviour (Shekhawat et al., 2021; Panseri et al., 2021). The calcium-phosphates material family is the most used, with hydroxyapatite (HA) and β-tricalcium phosphate (β-TCP) as forefathers. These materials, once implanted, provide an adequate environment enhancing cell attachment, proliferation, and differentiation (Panseri et al., 2021), determining bone regeneration.

The main properties of SGs are tuned based on the intended use of the bone graft, although it is often implanted with an internal fixation or plating device which further supports the bone graft from excessive loads during the callus remodelling and maturation phases. In particular, it is possible to identify two main types of applications within the human body: load-bearing districts (LBD) and non-load-bearing districts (NLBD). This separation in the intended use leads to a significant difference in the design of the scaffold, particularly regarding its mechanical properties. For LBD applications, the scaffold must present suitable mechanical properties, similar or superior to native bones, to ensure primary mechanical stability, avoiding abrupt ruptures that can lead to patient tissue damage and the need for revision surgery. Not only primary stability but also fatigue strength should be ensured by the device, which should withstand cyclic loads up to new bone formation and scaffold integration/resorption, which occurs mainly between 3 and 6 weeks based on the size of the defect and the properties of the implanted scaffold (Winkler et al., 2018; Wu et al., 2018).

To properly understand the potential efficacy of bone substitutes, it is fundamental to fully characterize the scaffold both under a morphological and mechanical point of view. This characterization would allow comparing their characteristics with bones and among themselves, based on the intended use and application site. It could be useful not only from a research point of view but also in the regulatory domain. Companies intending to bring medical devices like bone substitutes to the European Union market must adhere to the requirements outlined in the MDR 2017/745, corresponding to the device classification. In particular, bone grafts are typically classified as class III, due to their intended use and associated risks. Similarly, in the USA, to market a device, that does not require a Premarket Approval Application (PMA), it is mandatory to submit a 510(k) to the Food & Drug Administration (FDA). The 510(k) is a premarket submission used to prove the substantial equivalence between the device intended to be marketed and an already marketed device. The substantial equivalence regards both the intended use and technological characteristics of the two devices. When no substantial equivalence is observed, the applicant may submit a PMA. The free availability of 510(k) documents for several bone substitutes results being a great source of information regarding these medical devices.

The aim of this study is to present a systematic review of commercially available scaffolds with LBD intended use and how they are typically characterized from a morpho-mechanical point of view. Additionally, it is hypothesized that data about the morpho-mechanical properties of marketed bone grafts are under-reported and inhomogeneous.

2. Material and methods

2.1. Inclusion and exclusion criteria

Among all the available scaffolds present nowadays on the market, only the ones obeying the following criteria were included: (i) Cement or structured (granules, particles and blocks) bone grafts, (ii) available on the market and (iii) with LBD intended use. The above criteria included both biologized and non-biologized bone grafts and all bone grafts that (a) are mainly used in NLBDs and (b) are not available on the market because still at the research stage, were excluded.

2.2. Literature search

Two databases and one web research engine were retrospectively consulted for the present review in the period from December 2023 up to August 2024: the medical device database of the U.S. FDA (Premarket Approvals), PubMed and Google/Google Scholar. While for the former database, only the brand name of the scaffold was used, for the other two tools keywords were also added to reduce the number of scientific papers and focus the review on the morpho-mechanical characteristics of the bone grafts. In particular, the following keywords were used: “Strength”, “Permeability”, “Porosity”, “Osteoconductivity”, “Osteoinductivity” and “Biodegradability”. By applying the above-mentioned keywords, only papers reporting biological performances, intended as obtained from both human and animal studies, and the morpho-mechanical characterization of the commercially available scaffolds were obtained. Furthermore, only papers written in English, Italian, Spanish, German and French were considered eligible. The full text of the obtained papers was read by one researcher (D.N.).

2.3. Data organization and analysis

All retrieved data were collected in tables divided into Allograft, XGs and SGs, reporting some general information: manufacturer, material, form (i.e. block, granules, microchips, putty …, Fig. 1a), intended use (i.e. oral/cranio-maxillo-facial or Oral/CMF, orthopaedic/spine Fig. 1b) and mechanism of action (osteogenetic ‘OG’, osteoinductive ‘OI’, osteoconductive ‘OC’, biodegradable ‘BD’). Whenever possible, the information regarding material, form and intended use was collected from the 510(k) reports, otherwise appropriate scientific papers and/or brochures were found. In some cases, the manufacturer’s website was consulted and its statements regarding the corresponding bone substitute were considered. When this latter strategy was followed, in the reference column was added the acronym ’*ms*’ (i.e. manufacturer statement).

Also, morpho-mechanical characteristics were collected, in particular: porosity, type of mechanical test performed (Fig. 1c), strain rate, elastic/shear modulus, ultimate stress and permeability. These parameters were chosen looking at the typical external conditions experienced by the implanted bone grafts in terms of mechanical loadings (mechanical tests, strain rate, elastic/shear modulus, ultimate stress) and human cell colonization (porosity and permeability). Furthermore, these parameters were confirmed by available standards on bone grafts, which present how to measure the main properties of this type of device. In the last column of the table presenting the morpho-mechanical characteristics of the bone grafts, it is indicated where the corresponding data are exploited in the subsequent plots.

Regarding porosity, the bone grafts have been divided into three main groups based on the level of porosity: low, medium and high. In particular, the first group belongs to bone grafts with a porosity lower than 20%. The high porosity group is composed of devices with a porosity higher than 60% and finally, the medium group is in-between the other two (20%<porosity<60%).

The collected data were further analyzed to report the dependence of bone grafts’ morphology on intended use. To do so, it is fundamental to collect data on bone morphology derived from different human body districts. In particular, a total of 16 studies were considered, presenting data on bone volume fraction (BV/TV) for 5 human body districts: femur (Perilli et al., 2008a; Ohman et al., 2007a; Nikodem, 2012), tibia (Ding et al., 1997a; Lancianese et al., 2008), spine (Dempster et al., 1993; Teo et al., 2006; Follet et al., 2011a; Cendre et al., 1999a; Fyhrie et al., 1995), Iliac crest (Thomsen et al., 2002; Rothweiler et al., 2022) and jaw (O’Mahony et al., 2000; Giesen and van Eijden, 2000; Moon et al., 2004; Kim et al., 2013). Based on the fact that the BV/TV indicates the percentage of bone present in a unit of volume, it was obtained the value of

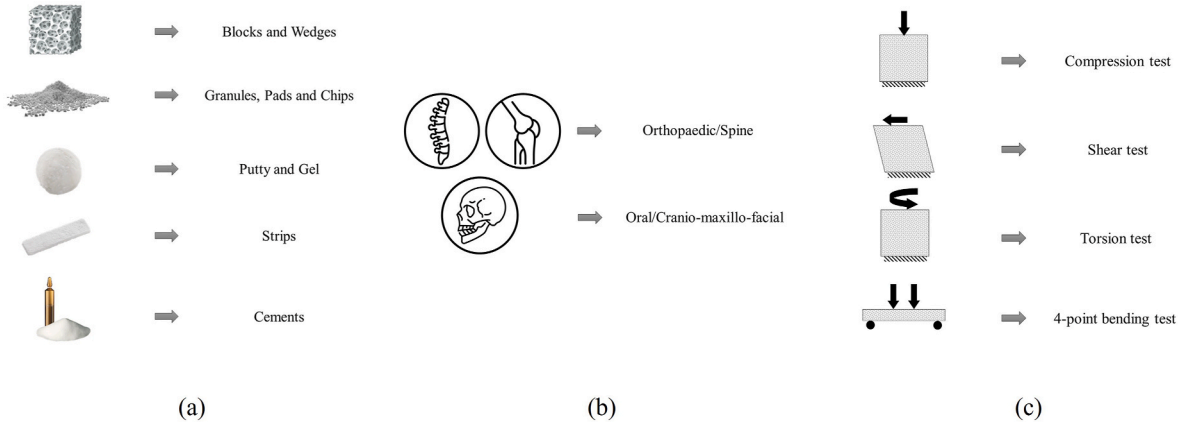

Fig. 1. Resume of scaffold grafts' forms considered in the present review (a), scaffold's intended use (b) and the mechanical test exploited to characterize them (c).

porosity as a complement to 100 of BV/TV. Finally, also the relationship between porosity and compressive strength, and the comparison from a general morpho-mechanical point of view between grafts and human bone was performed. The morpho-mechanical data regarding human bone were collected by looking at studies dealing with the correlation between mechanical properties and morphology of trabecular bone (Ding et al., 1997b; Ohman et al., 2007b; Follet et al., 2011b; Cendre et al., 1999b; Wu et al., 2021; Perilli et al., 2008b). From these studies, a linear relationship between bone volume fraction (BV/TV) and compressive strength of trabecular bone was found and exploited to define the corresponding BV/TV (C-BV) for the bone grafts. C-BV is the value of BV/TV which trabecular bone would present for a specific value of compressive strength.

3. Results

A total of 62 bone substitutes, from 37 different companies, were selected and divided into three main groups, based on their origin: Allograft (n = 5), Xenograft (n = 14) and Synthetic grafts (n = 43). In Fig. 2 is graphically outlined the methodological selection process of the useful records according to PRISMA guidelines. A total of 140 scientific papers, 24 brochures and 32 510(k) documents have been selected for the present review, starting from an opening balance of 3467 records.

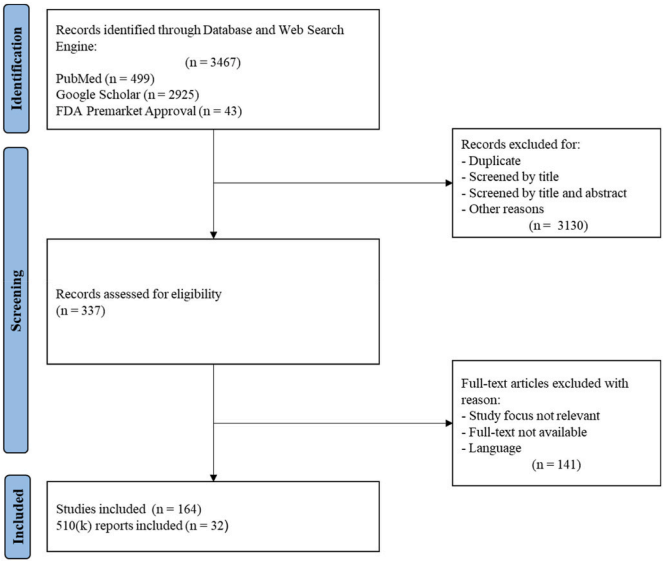

Fig. 2. Flow diagram of the literature selection procedure.

3.1. General information

In Table 1, 2a and 2b are resumed the basic information of the allografts, XGs and SGs here considered.

3.1.1. Allografts

Material. Allografts differ from one another because of the various human tissues used or the methods used during processing. In terms of material, it is observed that all the considered allografts, with the exception of Dynagraft®, are obtained from human cancellous bone. Dynagraft® could be obtained indifferently from cortical and cancellous human bone. Furthermore, Dynagraft® is presented in two main compositions: a demineralized bone structure with collagen or a poloxamer carrier within which demineralized human bone particles are dispersed. A different composition is observed for INFUSE®, which is composed of human collagen sponge enriched with rhBMP-2, which is an osteoinductive bone growth factor obtained from human bone. Not only the material but also the processing technique is different between allografts. For example, even if Maxgraft®, Osteosponge® and Osteocel® are all derived from human trabecular bone, the latter two are subjected to traditional demineralization while the former is subjected to a patented cleaning process (Allotec® process).

Form. Due to their origin, allografts are mainly presented in the form of solid scaffold (i.e. blocks, granules, disks). In some cases, as for INFUSE® Bone graft and Dynagraft®, putties are preferred exploiting human collagen or poloxamers as carriers within which particles of human bone or proteins are dispersed.

Intended use. The considered allografts are intended for two main applications: orthopaedic/spine and maxillofacial. In particular, all the allografts, but Maxgraft®, are intended to be used in orthopaedic/spinal surgery, with the case of INFUSE® Bone Graft which could be also used for oral and cranio-maxillofacial applications.

Mechanism of action. Thanks to their human-derived nature, all allografts are osteoconductive, osteoinductive and bio-degradable, while osteogenesis is indicated only for INFUSE® Bone graft, Osteosponge® and Osteocel.

3.1.2. Xenografts

Material. It was observed that in most cases XGs are obtained from bovine bone. But other animal species are also exploited for Biocoral®, Bonemedik-S and ProOsteon® 500R which are coralline-derived, Osteoplant® which is equine-derived and MinerOss® XP which is obtained from porcine bone. In particular, coralline-derived bone grafts are composed of coralline calcium carbonate which is added hydroxyapatite in the case of Bonemedik-S and ProOsteon® 500R. Instead, Osteoplant® is obtained through a particular process, called ZymoTeck® process, from equine bone, both cortical and cancellous (harvest

Table 1
Main properties of allografts and xenografts, indicating the manufacturer, material, form, intended use and mechanism of action.

Product Name	Manufacturer	Material	Form	Intended Use	Mechanisms of Action	Ref
ALLOGRAFTS						
Dynagraft®	IsoTis, Inc.	Poloxamer carrier (Putty and Gel) or Collagen (Block) with DFDBA			OI[a],OC and BD	Urrutia et al., 2008; Yao and Ho, 2009; Coulson et al., 1999; Dinopoulos and Giannoudis, 2006; 510(k) no. K040419 and *ms*
INFUSE® Bone Graft	Medtronic, Inc.	Collagen sponge carrier with rhBMP-2			OG, OI[a], OC and BD	510(k) no. P050053; Cottrill et al., 2023; McKay and Sandhu, 2002 and *ms*
Maxgraft®	Botiss biomaterials GmbH	Human Bone – subjected to Allotec® process			OI[a],OC and BD	botiss biomaterials GmbH, 2023; Solakoğ et al., 2022; Kloss et al., 2023; Lorenz et al., 2017 and *ms*
Osteosponge®	Xtant Medical Holdings, Inc.	Human Bone – Demineralized			OG, OI[a], OC and BD	Miller et al., 2012; Berberi et al., 2014; Bhamb et al., 2019 and *ms*
Osteocel	Nuvasive, Inc.	Human Bone – Demineralized			OG, OI[a], OC and BD	Steijvers et al., 2022; Ammerman et al., 2013 and *ms*
XENOGRAFTS						
Biocoral®	Inoteb	Coralline calcium carbonate			OC and BD	Giuliani et al., 2014; Bio Coral Calcium Bone, 2019
Bio-Oss®	Geistlich Pharma AG	Bovine Bone - Sintered			OC and BD	510(k) no. K122894; Sartori et al., 2003; Jensen et al., 2012
Bonemedik-S	Meta Biomed Co. Ltd.	Coralline calcium carbonate and HA			OC and BD	510(k) no. K070897; Meta Biomed Co. ltd, 2014
Cerabone®	Botiss biomaterials GmbH	Bovine Bone - Demineralized			OC	Institut Straumann AG, 2017; 510(k) no. K173594; Van der Stok et al., 2011; Zhang et al., 2019 and *ms*
Collapat® II	Zimmer Biomet Holdings, Inc.	Bovine collagen type I and HA granules			OC and BD	Haenle et al., 2013 and *ms*
Endobon®	Zimmer Biomet Holdings, Inc.	Bovine Bone - Demineralized			OC	510(k) no. K980779; Spies et al., 2010
Healos®	DePuy Synthes Inc	Bovine collagen type I and HA matrix			OC and BD	Ploumis et al., 2010; Neen et al., 2006; 510(k) no. K012751; 510(k) no. K062495; DePuy Spine, 2023
MinerOss® XP	BioHorizons®	Porcine bone – Processed			OC and BD	Krennmair et al., 2023; Chang, 2021
Orthoss®	Geistlich Pharma AG	Bovine Bone - Processed			OC and BD	Geistlich Pharma, 2005; Dorati et al., 2014; 510(k) no. K190754
Osteoplant®	Bioteck S.p.A.	Equine Bone with type I collagen– subjected to Zymo-Teck® process			OI[a], OC and BD	Sollazzo et al., 2010a; Lauritano et al., 2012
Pyrost®	Stryker Corp.	Bovine Bone - Deproteinized and sintered			OC	Tsuang et al., 1997; Perlick et al., 2001
ProOsteon® 500R	Zimmer Biomet Holdings, Inc.	Coralline calcium carbonate and HA			OC and BD	510(k) no. K980817; Biomet, 2018
Smartbone®	IBI SA	Bovine Bone - Decellularized and deproteinized (reinforced with polymers and collagen)			OI[a], OC and BD	IBI SA, 2015; D'Alessandro et al., 2017; Grottoli et al., 2019
Surgibone®	Unilab, Inc.	Bovine Bone - Partially deproteinized and processed			OC and BD	Balakrishnan et al., 2000; Cabbar et al., 2011

[a] Osteoinduction was declared by the manufacturer or found in scientific papers.

from different animal sites, from femur to homerus) and MinerOss® XP is obtained from porcine bone subjected to demineralization. The rest of the xenografts are made of either bovine bone matrix (cancellous bone) subjected to a process of demineralization/deproteinization (Bio-Oss®, Cerabone®, Endobon®, Orthoss®, Pyrost®, Smartbone® and Surgibone®) or bovine collagen type I with HA (Collapat® II and Healos®). Of particular interest is Smartbone®, which is composed by a decellularized bovine bone matrix reinforced with polymers and collagen. In this latter case, the graft is indicated as xenohybrid.

Form. In terms of forms, xenografts are mainly presented in

Table 2a
Resume of the main properties of SGs, indicating the manufacturer, material, form, intended use and mechanism of action. ACP = Amorphous calcium phosphate; Bis-GMA = bisphenol A-glycidyl methacrylate; CDA = Calcium deficient apatite; DCP = dicalcium phosphate; DCPA = anhydrous dicalcium phosphate; DCPD = dicalcium phosphate dihydrate; DMPT = N,N-dimethyl-p-toluidine; HPMC = hydroxypropyl methylcellulose; HQ = hydroquinone; PMMA = polymethyl methacrylate; MMA = Methyl methacrylate; MCPM = monocalcium phosphate monohydrate; TCP = tri-calcium phosphate; TeCP = tetracalcium phosphate monoxide; TTCP = tetracalcium phosphate.

SYNTHETIC GRAFTS

Product Name	Manufacturer	Material	Form	Intended Use	Mechanisms of Action	Ref
Affinos®	Kuraray Co., Ltd.	β-TCP			OC and BD	Ikuta et al., 2022; Noguchi et al., 2019
Alliment®	Beijing Bonsci Technology Co. Ltd.	Powder: PMMA, $C_{14}H_{10}O_4$ and $BaSO_4$ Liquid: MMA, DMPT and HQ			*n.a.*	Feng et al., 2021 and *ms*
b.BONE™	GreenBone Ortho S.p.A.	HA and β-TCP			OI*, OC and BD	Kon et al., 2021; Tampieri et al., 2019; GREENBONE ORTHO, 2023; Alt et al., 2023
Bicera™	Wiltrom Co., Ltd.	HA and β-TCP			OC and BD	Chen et al., 2017; Chen et al., 2012; 510(k) no. K110949
Biobase®	Biovision, Inc.	α-TCP			OC and BD	Kü et al., 2004; Seebach et al., 2010; Biomaterial, 2022a, 2022b and *ms*
Biobon®/α-BSM	Zimmer Biomet Holdings, Inc.	Powder: ACP and DCPD Liquid: aqueous saline solution			OC and BD	Spies et al., 2009; Kuemmerle et al., 2005; 510(k) no. K091729; Heini and Berlemann, 2001
Biopex®-R	MitsubishiPharma Corporation	Powder: α-TCP, DCPD and TeCP Liquid: H_2O, $C_4H_4Na_2O_4$ and $C_{14}H_{22}NNaO_{16}S$			OC and BD	Kurashina et al., 1995; Saijo et al., 2008; Nakadate et al., 2008 and *ms*
Biosorb®	SMB Holding SA	β-TCP			OC and BD	510(k) no. K061022; Saragaglia et al., 2011; Galois et al., 2002
Bonesave®	Stryker Corp.	HA and β-TCP			OC and BD	510(k) no. K033258; Gagala, 2021; Blom et al., 2005; Blom et al., 2009
BoneSource®	Stryker Corp.	TTCP and DCP			OC and BD	Rupprecht et al., 2003; 510(k) no. K031435
Calcibon® (ex. Biocement D)	Zimmer Biomet Holdings, Inc.	Powder: α-TCP, DCPA, $CaCO_3$ and HA Liquid: Na_2HPO_4			OC and BD	Mai et al., 2008; Friesenbichler et al., 2017
Calcigen® S	Zimmer Biomet Holdings, Inc.	Powder: CaH_4O_6S Liquid: set solution			OC and BD	510(k) no. K013790 and *ms*
Cementek®	Teknimed	Powder: α-TCP, TTCP and $C_3H_7Na_2O_6P$ Liquid: $Ca(OH)_2$ and H_3PO_4			OC and BD	Spies et al., 2010
Ceraform®	Teknimed	β-TCP and HA			OC and BD	510(k) no. K040669; Botez et al., 2009
Cerament®	Bonesupport Holding AB	Powder: HA and $CaSO_4$ Liquid: iohexol			OC and BD	510(k) no. K201535; Iundusi et al., 2015; Guarnieri et al., 2013
ChronOS® Inject	DePuy Synthes Inc	Powder: β-TCP, MCPM, β-TCP granules and $MgHPO_4$ Liquid: solution of sodium hyaluronate			OC and BD	Joeris et al., 2010; Schrö et al., 2020; Synthes GmbH
Collagraft®	Zimmer Biomet Holdings, Inc.	HA, TCP and type I bovine dermal collagen			OC and BD	Cornell et al., 1991; Leupold et al., 2006
CortOss®	Orthovita, Inc.	Bis-GMA			OC and BD	Granville and Jacobson, 2017; Palussiè et al., 2005; 510(k) no. K080108; Sanus et al., 2008
Engipore®	Finceramica S.p.A.	HA			OC and BD	Sollazzo et al., 2010b; Fin-Ceramica Faenza
Eurobone®	Kasios, Inc.	Powder: β-TCP and $Na_2P_2O_7$ Liquid: H_2O, H_3PO_4 and H_2SO_4			OC and BD	Frayssinet et al., 2000; Kayal et al., 2021
Graftys® HBS	Graftys SA	Powder: α-TCP, DCPA, MCPM, CDA and HPMC Liquid: Na_2HPO_4			OC and BD	510(k) no. K082498; Le Ferrec et al., 2020 and *ms*
Graftys® Quickset	Graftys SA	Powder: α-TCP, DCPA, CDA and HPMC Liquid: Na_2HPO_4			OC and BD	Brueckner et al., 2019a and *ms*

* Osteoinduction was certified by the manufacturer (CE mark).

Table 2b
Resume of the main properties of SGs, indicating the manufacturer, material, form, intended use and mechanism of action. DCPD = dicalcium phosphate dihydrate; DMPT = N,N-dimethyl-p-toluidine; HQ = hydroquinone; MCPM = monocalcium monohydrate; MMA = Methyl methacrylate; PGA = polyglycolide acid; PLG = poly D, L -lactide-co-glycolide; PMA = polymethil acrylate; PMMA = polymethyl methacrylate; PVP = polyvinylpurrolidone; TCP = tri-calcium phosphate; TTCP = tetra-calcium phosphate.

SYNTHETIC GRAFTS

Product Name	Manufacturer	Material	Form	Intended Use	Mechanisms of Action	Ref
HydroSet®	Stryker Corp.	Powder: TTCP and DCPD Liquid: H_2O, Na_2HPO_4, NaH_2PO_4 and PVP			OC and BD	Clarkin et al., 2009; 510(k) no. K161447; Hannink et al., 2008
IngeniOS® β-TCP	Zimmer Biomet Holdings, Inc.	Silicated β-TCP			OC and BD	Moustafa et al., 2015; Zimmer Biomet Dental
IngeniOS® HA	Zimmer Biomet Holdings, Inc.	HA			OC	Greenspan, 2013 and *ms*
Macrobone®	Euroteknika Group	β-TCP			OC and BD	Berberi et al., 2014, Euroteknika
MagnetOs® Granules	Kuros Biosciences BV	TCP and HA			OI*, OC and BD	van Dijk et al., 2023a; van Dijk et al., 2023b; 510(k) no. K213111
Mastergraft® Matrix EXT	Medtronic, Inc.	HA, TCP and type I lyophilized collagen			OC and BD	510(k) no. K141824; Sofamor Danek, 2005
Maxresorb®	Botiss biomaterials GmbH	HA and β-TCP			OC and BD	Bielenstein et al., 2022; botiss biomaterials GmbH
MBCP®	Biomatlante SA	HA and β-TCP			OI*, OC and BD	Daculsi et al., 2013; Daculsi et al., 2008; 510(k) no. K032268
MIIG® X3	Stryker Corp.	$CaSO_4$			OC and BD	Yu et al., 2009; Changoor et al., 2006; Wright Medical Technology, 2012
Mimix®	Zimmer Biomet Holdings, Inc.	Powder: TTCP/α-TCP and $C_6H_9Na_3O_9$ Liquid: $C_6H_8O_7$ and H_2O			OC	Mann et al., 2011; Goebel and Jacob, 2005; 510(k) no. K043280
Norian® SRS®	DePuy Synthes Inc	Powder: α-TCP, $CaCO_3$ and MCPM Liquid: solution of sodium phosphate			OC and BD	Schrö et al., 2020, 510(k) no. K011897; Synthes ® and Inc, 2006a; Synthes ® and Inc, 2006b
Osferion®	Olympus Terumo Biomaterials Co.	β-TCP			OI*, OC and BD	Yamasaki et al., 2009; 510(k) no. K061499; Kondo et al., 2006
OsSatura® BCP	IsoTis, Inc.	HA and TCP			OC and BD	510(k) no. K030131
Osteopal V®	Heraeus Medical GmbH	Powder: PMA, PMMA, ZrO_2 and $C_{14}H_{10}O_4$ Liquid: MMA, DMPT and HQ			*n.a.*	Galovich et al., 2011; Heraeus Medical GmbH, 2020
Osteoset®	Stryker Corp.	$CaSO_4$			OC and BD	Chen et al., 2006; Wright Medical Technology, 2021
Ostim®	Heraeus Medical GmbH	HA			OC and BD	510(k) no. K030052; Huber et al., 2008; Schwarz et al., 2006; Heraeus, 2008
Stimulan® Rapid Cure	Biocomposites, Inc.	$CaSO_4$			OC and BD	Kallala et al., 2018a, 2018b; 510(k) no. K141830 and *ms*
SuperPore®	Hoya Technosurgical Corporation	β-TCP			OC and BD	Seto et al., 2013 and *ms*
Triosite®	Zimmer Biomet Holdings, Inc.	β-TCP and HA			OC and BD	Chen et al., 2012, 2017, Zimmer GmbH
TruFit®	Smith & Nephew, Inc.	PLG, $CaSO_4$, PGA fiber and sulfactant			OC and BD	Melton et al., 2010a; Boffa et al., 2021; Niederauer et al., 2006; 510(k) no. K040047

(*continued on next page*)

Table 2b (*continued*)

SYNTHETIC GRAFTS						
Product Name	Manufacturer	Material	Form	Intended Use	Mechanisms of Action	Ref
Vertebroplastic®	DePuy Synthes Inc	Powder: MMA and $BaSO_4$ Liquid: MMA			*n.a.*	Handal et al., 2011; 510(k) no. K201831

* Osteoinduction was declared by the manufacturer or found in scientific papers.

structured shapes, with 11 over 14 xenografts delivered in the form of blocks and 10 of those are also sold in granules (only MinerOss® XP is delivered exclusively in the form of granules). Only Collapat® II is presented in the form of putty, as a consequence of the combination of bovine collagen and HA in granules, while Healos® is also sold in the form of a deformable strip.

Intended use. Based on the fact that most of the considered xenografts are delivered in the form of blocks, they are mainly used in the orthopaedic/spine surgery field as bone void filler and extenders. Only 4 XGs presented exclusively Oral/Cranio-maxillo-facial as intended use (Bio-oss®, Cerabone®, Endobon®, MinerOss® XP), while 6 XGs presented both Ortho/spine and Oral/CMF indications.

Mechanism of action. Thanks to their origin, all the xenografts are osteoconductive, but in contrast to allografts, most of them are not osteoinductive, with the exception of Osteoplant® and Smartbone®. Furthermore, all xenografts but Cerabone®, Endobon® and Pyrost® are bio-degradable. In particular, the lack of degradability of Endobon® is intentionally designed for its application, while Cerabone® presents only superficial absorption to help graft osteointegration.

Table 3
Morpho-mechanical data of XGs in terms of porosity, mechanical test performed, strain rate, elastic/shear modulus, ultimate stress and permeability. The last column indicates whether the data regarding the corresponding grafts have been used also in the subsequent graphs.

XENOGRAFTS										
Product Name	Porosity (%)	Mechanical Test 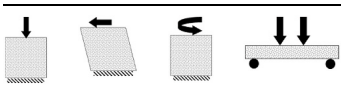				Strain rate (s^{-1})	Elastic/ Shear Modulus (GPa)	Ultimate stress (MPa)	Permeability (10^{-10} m^2)	Ref	Exploited in Figure
Biocoral® - A	20–30	✓				n.a.	21.3–27.9	78–142	44.6	Demers et al., 2002; Decambron et al., 2017	3,4a,5
Biocoral® - P	47–51	✓				n.a.	7.6–8.4	20–31	1.2	Demers et al., 2002; Decambron et al., 2017	3,4a,5
Bio-Oss®	70	✓				0.001	2.9 ± 0.7	0.34 ± 0.15	25.5	Ott et al., 2017; Marcos et al., 2019	3,4a,5
Bonemedik-S	70	✓				n.a.	n.a.	4	n.a.	*Ms*	3,4a,5
Cerabone®	65–80	✓				n.a.	n.a.	4.2–5.6	6	Institut Straumann AG, 2017, Van der Stok et al., 2011; Zhang et al., 2019	3,4a,5
			✓			n.a.	n.a.	1.2–3.4			
Collapat® II	n.a.	n.a.				n.a.	n.a.	n.a.	n.a.	–	–
Endobon®	55–85	✓				0.0002	0.2–3.1	1–11	n.a.	Hing et al., 1999; Hing, 2005	3,4a,5
Healos®	95–99	✓				n.a.	n.a.	n.a.	n.a.	Neen et al., 2006, Baskin et al., 2012	–
MinerOss® XP	88–95			n.a.		n.a.	n.a.	n.a.	n.a.	Krennmair et al., 2023	3
Orthoss®	60–80	✓				0.004	n.a.	0.9–2.3	n.a.	Dorati et al., 2014, Gordon, 2005; Fassina et al., 2010	3,4a,5
Osteoplant®	65–82	✓				0.008	0.15 ± 0.07	11.3 ± 8.9	n.a.	Falvo D'Urso Labate et al., 2016	3, 5
ProOsteon® 500R	60–70	✓				0.0002	2.9 ± 1.3	5.87 ± 1.92	4.94 ± 1.91	Haddock et al., 1999	3,4a,5
Pyrost®	70	✓				n.a.	n.a.	n.a.	n.a.	Lauritano et al., 2012	3
Smartbone®	68.9 ± 2.8	✓				0.02	1.3 ± 0.2	25.8 ± 7.9	2.3 ± 3.4	IBI SA, 2015, Massini, 2022; Perale et al., 2019	3,4a,5
				✓		0.02	0.3 ± 0.1	23.8 ± 4.2			
					✓	0.02	0.5 ± 0.1	25.5 ± 4.4			
Surgibone®	n.a.	✓				0.001	n.a.	32.8	n.a.	Hess et al., 1995	5

3.1.3. Synthetic grafts

Material. The considered SGs could be divided in two main groups, based on their material family: polymeric or ceramic. The former group counts only for the 12% (5 over 43 SGs: Alliment®, CortOss®, Osteopla®V, TruFit® and Vertebroplastic®), in which three of them are principally made of PMMA. For the grafts of the latter group, two main phases of calcium phosphate are used, HA and β-TCP. In particular, 7 SGs are composed by pure β-TCP (Affinos®, Biosorb®, Chronos® Bone void filler, IngeniOS® β-TCP, Macrobone®, Osferion®, and SuperPore®), 3 SGs are made of pure HA (Engipore®, IngeniOS® HA and Ostim®) and 10 SGs are biphasic HA + β-TCP (b.BONE™, Bicera™, BoneSave®, Ceraform®, MagetOS® Granules, Maxgraft® Matrix EXT, Maxresorb®, MBCP®, OsSatura® BCP and Triosite®). It is worth also highlighting the use of α-TCP for Biobase®. α-TCP and β-TCP are also used in combination with other composites as powder components of cement, as in the case of Calcibon®, Eurobone® and Graftys® Quickset. Finally, it is interesting to notice that there are two SGs (Collagraft® and Maxgraft® Matrix EXT) whose biphasic ceramic matrix is filled with type I bovine dermal collagen and type I lyophilized collagen, respectively. The addition of type I collagen allows to obtain a structure similar to bone, as type I collagen is almost 90% of the organic constituent of human bone. Furthermore, it determines an osteoblast-friendly environment which increases the osteoinductivity of the bone substitute when combined with bone marrow (Mallick et al., 2022; Alvis et al., 2000).

Form. With respect Allografts and XGs, which are mostly supplied as blocks and granules, SGs allows to obtain cements, by mixing the powder (polymeric or ceramic) with a liquid component. In particular, over 43 bone grafts, the majority of the SGs are supplied in the form of granules (22 over 43), while16 are delivered in the form of cement and only 13 grafts are in the form of blocks. Finally, only Calcigen® S, Collagraft®, CortOss®, MIIG® X3 and Ostim® are available as putties. It is worth to highlight that in several cases the same SG is supplied in different forms.

Intended use. The majority of the SGs present as intended use the bone void and gaps filling in orthopaedic (i.e. extremities, pelvis etc.) and spine surgery (37 over 43). Only 10 grafts presented oral/CMF indication (Biobase®, Biobon®, Biopex®-R, Hydroset®, IngeniOS® β-TCP, IngeniOS® HA, Macrobone®, Maxresorb®, Mimix® and Ostim®).

Mechanism of action. With respect allografts, synthetic grafts typically do not present osteoinductive properties, with the exception of b.BONE™, Osterion®, MBCP® and MagnetOs® Granules, which, accordingly to literature, present an osteoinductive effect, intended as "passive" osteoinduction (Daculsi et al., 2013). Nevertheless, all SGs are osteoconductive but Alliment®, Osteopal® and Vertebroplastic®, which no information regarding their mechanism of action was found. Furthermore, with the exception of IngeniOS® HA and Mimix®, all SGs are bio-degradable.

3.2. Morpho-mechanical characteristics

The morpho-mechanical characteristics of the considered marketed bone substitutes are collected in Tables 3 and 4, whenever available. No description of either the morphological or the mechanical properties of allografts was found.

3.2.1. Xenografts

Porosity. Most of the considered XGs belonged to the high-porosity group, with a mean porosity near 70%. Only Biocoral®, whose two typologies Biocoral®-A and Biocoral®-P presented a mean porosity of 25 and 49% respectively, belongs to the medium-porosity subgroup. Regarding Surgibone®, and Collapat II no information regarding porosity was found. Some XGs presented high data dispersion. For example, Endobon®'s porosity ranged between 55 and 85%, resulting in the widest range observed for these grafts. At second place there was Osteoplant® with a porosity ranging from 65 to 82%, similar to Cerabone® (65–80%) and Orthoss® (60–80%).

Mechanical Test. From a mechanical characterization point of view, all except Collapat® II, Healos®, MinerOss® XP and Pyrost®, have been tested in compression and only Cerabone® and Smartbone® were also tested for different loading conditions: shear (Cerabone®) and 4-point bending and torsion (Smartbone®). For the tested xenografts, compressive strength (i.e. ultimate stress) ranged between 0.34 MPa (Bio-Oss®) and 110 MPa (Biocoral®-A). This wide range of values is sharply reduced considering exclusively bovine-bone derived xenografts, with the same minimum value (0.34 MPa), but a maximum compressive strength of 25.8 MPa (Smartbone®). Furthermore, only for few XGs also the compressive Young's modulus was presented, with a value of 24.6 ± 4.7 GPa, 8 ± 0.5 GPa, 2.9 ± 0.7 GPa, 1.6 ± 2.2 GPa, 0.15 ± 0.07 GPa, 2.9 ± 1.3 GPa and 1.3 ± 0.2 GPa for respectively Biocoral®-A, Biocoral®-P, Bio-Oss®, Endobon®, Osteoplant®, ProOsteon® 500R and Smartbone®. Finally, it is worth to highlight that in several cases no clear definition of the testing conditions and protocols was found. As a matter of fact, no information about the strain rate or the testing method was presented. However, from the available studies, it was found that the xenografts were tested at a strain rate ranging from 0.0001 to 0.02 s^{-1}.

Permeability. If few data were available regarding the mechanical response of xenografts, even fewer have been found on their permeability. In particular, only 6 xenografts presented information regarding their capacity to be permeated by a fluid, with a permeability coefficient of 44.6, 1.2, 25.5, 6, 4.94 ± 1.91 and 2.3 ± 3.4 $\cdot 10^{-10}$ m^2 for respectively Biocoral®-A, Biocoral®-P, Bio-Oss®, Bonmedik-S, ProOsteon® 500R and Smartbone®. In all cases the coefficient of permeability was measured by exploiting an experimental test bench, but for Cerabone® which permeability was evaluated through a fluid-dynamic numerical model.

Finally, it is worth highlighting the behaviour of Biocoral® in its two sizes: Biocoral®-A and Biocoral®-P. It is interesting to notice that higher permeability was observed for the scaffold with lower porosity: 44.6 $\cdot 10^{-10}$ m^2 for Biocoral®-A which presented a mean porosity of 25% while Biocoral®-P presented a permeability coefficient of 1.2 $\cdot 10^{-10}$ m^2 with a mean porosity of 49%. Even if it could appear counterintuitive, it sheds light on the fact that the scaffold's permeability not only depends on the percentage of porosity, but also on the level of interconnectivity between the pores, the percentage of open pores with respect to closed pores, and the tortuosity of the structure (Li et al., 2003).

3.2.2. Synthetic grafts

Porosity. While the porosity of the xenografts is strictly related to the bone structure from which they are obtained, regarding SGs the morphology is either designed or obtained from the manufacturing process. The design of the structure is typically possible when using 3d printing, while exploiting different manufacturing processes less control is possible, especially when considering bone cements. Among the 43 SGs considered, 36 presented information regarding their porosity. In particular, to the low-porosity group belonged 5 SGs with a mean porosity ranging from 0.7% (MIIG®X3) to 7.5% (BoneSource®). Instead, of similar numerosity were the medium- and high-porosity groups, which accounted for respectively 17 and 15 SGs. In particular, the medium-porosity subdivision presented a mean porosity between 35% (Calcibon® and ChroOS® Inject) and 60% (b.BONE™ and OsSatura® BCP), while the high-porosity group presented a minimum mean porosity of 65% with Triosite® and a maximum mean porosity of 90% with Engipore® and Macrobone®.

Mechanical Test. In terms of mechanical characterization, only 33 SGs presented data regarding their mechanical response and among this group, only 4 SGs have been characterized, along with compression, for distinct loading conditions: Alliment® (compression and 4-point bending), CortOss® (compression, 4-point bending, and shear), Osteopal® V (compression, 4-point bending, and shear) and Vertebroplastic®

Table 4
Morpho-mechanical data of SGs in terms of porosity, mechanical test performed, strain rate, elastic/shear modulus, ultimate stress and permeability. The last column indicates whether the data regarding the corresponding grafts have been used also in the subsequent graphs.

SYNTHETIC GRAFTS										
Product Name	Porosity (%)	Mechanical Test 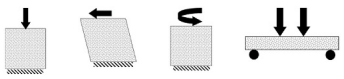				Strain rate (s^{-1})	Elastic/ Shear Modulus (GPa)	Ultimate stress (MPa)	Permeability (10^{-10} m^2)	Ref	Exploited in Figure
Affinos®	57 ± 5	✓				n.a.	n.a.	14.4 ± 2.6	n.a.	Noguchi et al., 2019	3,4b,5
Alliment®	n.a.	✓				0.035	n.a.	88.39 ± 5.29	n.a.	Feng et al., 2021	–
					✓	0.0002	3.28 ± 0.46	55.58 ± 4.27			
b.BONE™	60	✓				0.001	0.6	20.3	n.a.	Tampieri et al., 2019; GREENBONE ORTHO, 2023	3,4b,5
Bicera™	78–83	✓				n.a.	n.a.	1.8 ± 0.24	n.a.	Chen et al., 2017, 510(k) no. K110949	3,4b,5
Biobase®	53–63					n.a.	n.a.	n.a.	n.a.	Seebach et al., 2010	3
Biobon®/α-BSM	50–60	✓				n.a.	n.a.	4–9	n.a.	Spies et al., 2009, Saadalla et al., 2001	3,4b,5
Biopex®-R	40–50	✓				0.0006	n.a.	10[a]	n.a.	Kurashina et al., 1995, Schrö et al., 2020	3,4b,5
Biosorb®	30–50	✓				n.a.	n.a.	15.	n.a.	Galois et al., 2002, Passuti et al., 1997	3,4b,5
Bonesave®	50–55					n.a.	n.a.	n.a.	n.a.	Hing, 2005	3
BoneSource®	5–10	✓				0.001	0.474	5–34	n.a.	Miller et al., 2005; Van Lieshout et al., 2011	3,4b,5
Calcibon® (ex. Biocement D)	30–40	✓				0.001	0.79 ± 0.13	34 ± 6.8	n.a.	Van Lieshout et al., 2011; Blokhuis and Mallick, 2014; Kurien et al., 2013	3,4b,5
Calcigen® S	n.a.					n.a.	n.a.	n.a.	n.a.	–	–
Cementek®	50	✓				n.a.	n.a.	13–20	n.a.	Heini and Berlemann, 2001, He et al., 2014	3,5
Ceraform®	60–85	✓				n.a.	n.a.	<5	n.a.	Nich and Hamadouche, 2011	3,4b,5
Cerament®	40–50	✓				0.002	n.a.	7.3 ± 0.6	n.a.	Duncan and Sabatini, 2023; Dadkhah et al., 2016	3,4b,5
ChronOS® Inject	33–37	✓				0.001	n.a.	0.6–3	n.a.	Luo et al., 2016; Brueckner et al., 2019b	3,4b,5
Collagraft®	70.69 ± 6.52	✓				0.001	0.00127 ± 0.0001	0.31 ± 0.04	n.a.	Lee et al., 2006	3,4b,5
CortOss®	4.5 ± 2.5	✓				0.05	n.a.	146 ± 18	n.a.	Van Lieshout et al., 2011, Gheduzzi et al., 2006; DiCicco et al., 2003	3,4b
			✓			0.0001	5.51 ± 0.51	57 ± 10			
					✓	0.004	n.a.	8.4 ± 0.8			
Engipore®	90	✓				0.0005	0.24 ± 0.07	2.5 ± 0.8	1.07	Fin-Ceramica Faenza; Cunha et al., 2013; Tal et al., 2018	3,4b,5
Eurobone®	2.6 ± 0.7	✓				0.001	0.46 ± 0.096	10.5 ± 2	n.a.	Van Lieshout et al., 2011	3,4b,5

(continued on next page)

Table 4 (*continued*)

SYNTHETIC GRAFTS										
Product Name	Porosity (%)	Mechanical Test				Strain rate (s^{-1})	Elastic/ Shear Modulus (GPa)	Ultimate stress (MPa)	Permeability (10^{-10} m^2)	Ref	Exploited in Figure
		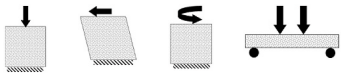									
Graftys® HBS	51.3 ± 1.2	✓				0.08	n.a.	14 ± 2	n.a.	Mellier et al., 2017	3,4b,5
Graftys® Quickset	52.6 ± 1.4	✓				0.08	n.a.	25 ± 5	n.a.	Mellier et al., 2017	3,4b,5
HydroSet®	2.9 ± 0.9	✓				0.001–0.0025	0.20–0.35	10–25	n.a.	Clarkin et al., 2009, Van Lieshout et al., 2011	3,4b,5
IngeniOS® β-TCP	75					n.a.	n.a.	n.a.	n.a.	Moustafa et al., 2015	3
IngeniOS® HA	70–80					n.a.	n.a.	n.a.	n.a.	Greenspan, 2013	3
Macrobone®	90					n.a.	n.a.	n.a.	n.a.	Berberi et al., 2014	3
MagnetOs® Granules	80					n.a.	n.a.	n.a.	n.a.	van Dijk et al., 2023	3
Mastergraft® Matrix EXT	80					n.a.	n.a.	n.a.	n.a.	Sofamor Danek, 2005	3
Maxresorb®	67.5 ± 3.6					n.a.	n.a.	n.a.	0.31	Zhang et al., 2019	3
MBCP®	70	✓				n.a.	n.a.	3.04 ± 0.79	n.a.	510(k) no. K032268	3,4b,5
MIIG® X3	0.7 ± 0.4	✓				0.001	0.67 ± 0.15	21.78 ± 4.82	n.a.	Van der Stok et al., 2011, Van Lieshout et al., 2011	3,4b,5
Mimix®	n.a.	✓				n.a.	n.a.	22.5	n.a.	Mann et al., 2011	–
Norian® SRS®	38–44	✓				0.001	0.67 ± 0.15	18–33	n.a.	Luo et al., 2016	3,4b,5
Osferion®	75 ± 3	✓				n.a.	n.a.	2–5	n.a.	Noguchi et al., 2019	3,4b,5
OsSatura® BCP	60					n.a.	n.a.	n.a.	3.5 ± 0.3	Li et al., 2003	3
Osteopal V®	3.55 ± 0.11	✓				0.05	n.a.	82 ± 3	n.a.	Gheduzzi et al., 2006) Lewis, 2000	3,4b
			✓			0.0001	3.5 ± 0.24	46 ± 8			
					✓	0.004	n.a.	6.8 ± 0.4			
Osteoset®	n.a.	✓				n.a.	n.a.	34.94 ± 4.04	n.a.	Urban et al., 2004	5
Ostim®	50.5 ± 4.5	✓				0.001	0.006 ± 0.003	0.24 ± 0.05	n.a.	Pawelke et al., 2023	3,4b
Stimulan® Rapid Cure	n.a.	✓				0.003	n.a.	5.05 ± 0.55	n.a.	Farrar, 2015	5
SuperPore®	75	✓				n.a.	n.a.	5–7	n.a.	Seto et al., 2013	3,4b,5
	67	✓				n.a.	n.a.	20	n.a.	*Ms*	
	57	✓				n.a.	n.a.	48	n.a.		
Triosite®	70	✓				n.a.	n.a.	2.6 ± 0.3	n.a.	Chen et al., 2017, Trecant et al., 1994	3,4b,5
TruFit®	n.a.	✓				n.a.	0.05–0.08	5.5–8.5	n.a.	Melton et al., 2010	5
Vertebroplastic®	n.a.	✓				0.05	n.a.	70 ± 4	n.a	Gheduzzi et al., 2006	–
			✓			0.0001	2.57 ± 0.20	45 ± 5			
					✓	0.004	n.a.	7 ± 0.2			

[a] At 3h exposure to simulated body fluid.

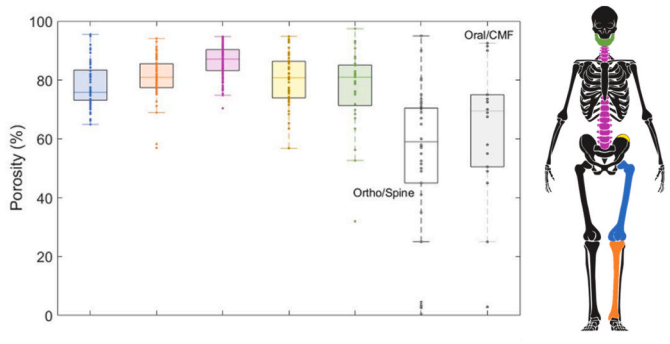

Fig. 3. Porosity distribution (%) of human trabecular bone for different representative body sites: femur (blue), tibia (orange), spine (purple), iliac crest (yellow) and jaw (green). Porosity data for bone grafts with intended use in ortho/spine field are represented in white with black contour while bone grafts used in the oral/CMF (cranio-maxillofacial) field are represented in grey.

(compression, 4-point bending, and shear). Following the subdivision previously presented between polymer-based and ceramic-based SGs, it was possible to analyse the mechanical properties of these grafts. In particular, the former group presented a mean compressive strength which varies from 7 MPa (TruFit®) to 146 MPa (CortOss®). However, excluding TruFit® which presented particularly low mechanical properties, the rest of the polymer-based SGs presented similar mechanical responses: 82 MPa, 88.39 MPa and 70 MPa compressive strength for respectively Alliment®, Osteopal V® and Vertebroplastic®. With the exception of TruFit®, which presented a Young's Modulus between 50 and 80 MPa, no information was found on the elastic modulus for polymer-based SGs. Alliment® CortOSS®, Osteopal V® and Vertebroplastic® were all characterized also in 4-point bending and the latter three were also tested in shear resulting respectively in a bending strength of 55.6 ± 4.3 MPa, 57 ± 10 MPa, 46 ± 8 MPa and 45 ± 5 MPa and a shear strength of 8.4 ± 0.8 MPa 6.8 ± 0.4 MPa and 7 ± 0.2 MPa.

Moving to the ceramic-based SGs, for a total of 28 over 38 grafts were found data on their mechanical behaviour, but all exclusively regarding compressive tests. In this regard, the value of compressive strength presented huge variability among the SGs, mainly due to differences in material and morphology. The compressive strength ranged between 0.24 MPa (Ostim®) and 48 MPa (SuperPore®). This latter SG is available in three sizes, based on the level of porosity: 57%, 67% and 75%, with the lower porosity level corresponding to the 48 MPa compressive strength. It was possible to deeply analyse the value of compressive strength by identifying subgroups presenting the same bulk material. In particular, three main subgroups have been easily identified: HA-bulk, β-TCP-bulk and biphasic-bulk (HA + β-TCP). To the first group belonged Engipore® and Ostim®, which presented respectively a compressive strength of 2.5 ± 0.8 MPa and 0.24 ± 0.05 MPa. For this group, it was found also information regarding their Young's Modulus, which was equal to 240 ± 7 MPa and 6 ± 3 MPa, respectively. The second group was composed of 4 SGs: Affinos®, Biosorb®, Osferion® and SupePore® (in its three sizes). For the first three SGs, the compressive strength respectively was equal to 14.4 ± 2.6 MPa, 12.5 ± 2.5 MPa, 3.5 ± 1.5 MPa while SuperPore® presented a strength of 6 ± 1 MPa, 20 MPa and 48 MPa for respectively a porosity of 75%, 67% and 57%. Finally, the biphasic-bulk group presented 4 SGs: b.BONE™, Bicera™, MBCP® and Triosite® with a compressive strength of 20.3 MPa, 2.6 ± 0.3 MPa, 3.0 ± 0.8 MPa and 1.8 ± 0.2 MPa, respectively.

Permeability. Few data were found regarding tests focusing on the permeability of SGs. In particular, only 3 SGs have been tested to find the coefficient of permeability, obtaining a mean value of 1.07, 0.31 and 3.5 ± 0.3 $\cdot 10^{-10}$ m^2 for respectively Engipore®, Maxresorb® and OsSatura® BCP. While for Engipore® and OsSatura® BCP, the permeability coefficient was evaluated through an experimental test bench, for Maxresorb® it was calculated by exploiting a fluid-dynamic numerical model.

3.3. Further analysis

3.3.1. Correlation between bone grafts' morphology and their intended use

From literature, the mean human bone's porosity resulted equal to 78%, 81%, 86%, 80% and 77% for respectively human femur, tibia, spine, Iliac crest and jaw (Fig. 3). From Fig. 3 it is possible to observe a high dispersion of data, especially for the jaw, which presents a standard deviation of 14%, with respect to a standard deviation of 7%, 7%, 5% and 8% for respectively human femur, tibia, spine and iliac crest. This higher dispersion regarding the human jaw is ascribable to the fact that some studies considered the lower jaw (O'Mahony et al., 2000; Giesen

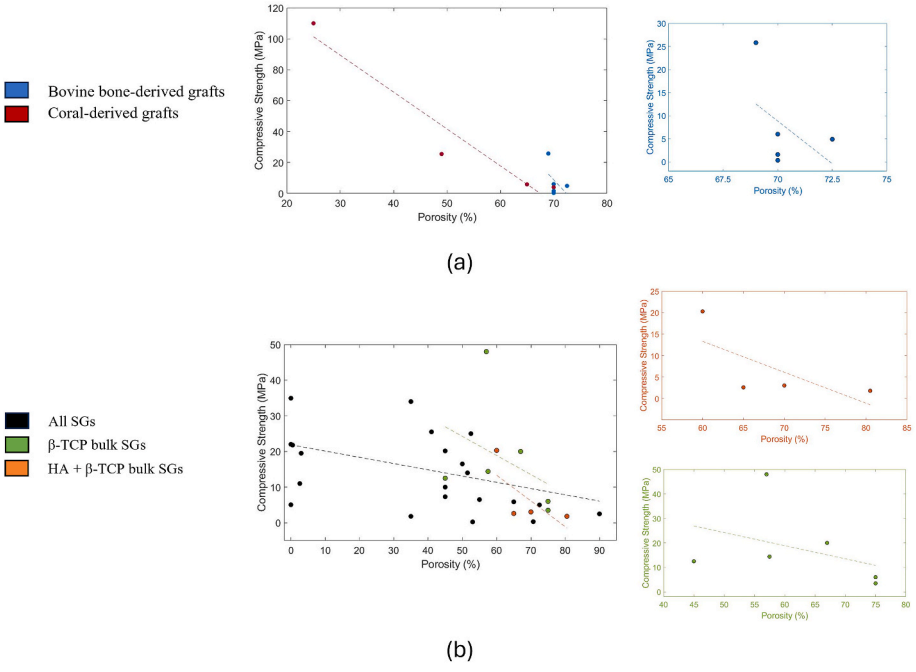

Fig. 4. Relationship between porosity and compressive strength for XGs (a) and for SGs (b).

and van Eijden, 2000; Moon et al., 2004) while others the upper one (Kim et al., 2013). Looking at the data collected (Tables 3 and 4) regarding both XGs and SGs, it appears clear that most of the bone grafts belong to the medium/high-porosity groups, either their intended use is the application in the oral/cranio-maxillofacial or in the orthopaedic/-spine surgery. In particular, among the whole bone grafts group reporting the values of porosity (n = 51) only 6 bone grafts belong to the low-porosity group and all present orthopaedic/spine surgery as intended use. A mean overall porosity of 54.6% ± 23.7% and 62.9% ± 22.8% is observed for respectively the grafts used for orthopaedic/spine and oral/CMF applications. High dispersion is observed for both groups due to the presence of grafts with both very low and very high porosity (i.e. for the ortho/spine group there is MIIG® X3 with a porosity of 0.7% and Healos® with a porosity of 95%). However, no significant difference was found between the ortho/spine and the oral/CMF groups ($p > 0.05$). Comparing grafts' porosity with human bone data results in a difference of about 32%, 35%, 39% and 35% between the mean porosity of the Ortho/Spine group and respectively the mean porosity of femur, tibia, spine and iliac crest. Considering the Oral/CMF group it was evaluated a difference of 21% with respect to data obtained from jaw bone.

3.3.2. Relationship between porosity and compressive strength

The relationship between porosity and mechanical properties is performed by comparing scaffolds with the same bulk material, to exclude the effect of the material on the values of compressive strength.

Xenografts The presented xenografts are derived from different animal species, but two main groups are identifiable for numerousness: bovine-derived and coral-derived xenografts. To find a relation between porosity and compressive strength (which was the most reported mechanical property) the two above-mentioned groups were considered separately. In Fig. 4a compressive strength is plotted against the corresponding value of porosity (whenever available) both for bovine- (n = 5) and coral-derived (n = 4) grafts. While for bovine-bone derived XGs no clear trend was observed, mainly due to the fact that all presented similar porosity and differences in the treatment/sterilization process, for the coral-derived grafts the trend was clearer. As expected, it was observed a decrease in the compressive strength of the grafts with an increase in porosity, passing from a compressive strength of 110 MPa for a porosity of 25 % (Biocoral®-A) to a value of 4 MPa, corresponding to a porosity of 70 % (Bonemedik-S).

Synthetic Grafts For what concern SGs, it was possible to observe a trend similar to XGs between porosity and compressive strength (which again was the most reported mechanical property). In particular, Fig. 4b shows the relation between the morphological and the mechanical parameter for all the SGs (no matter the bulk material) in dark, while in green and orange are highlighted the trends for two specific subgroups: β-TCP bulk (n = 6) and HA + β-TCP bulk (n = 4). Regardless of the low numerosity, high dispersion of the data and the poor correlation obtained, it was observed an overall decreasing trend in the value of compressive strength following an increase in the porosity. This behaviour was particularly significant looking at the two subgroups. Greater fitting of the linear interpolation curve was observed for the HA+ β-TCP -bulk subgroup, while more dispersed data were obtained for the pure β-TCP-bulk grafts. Nevertheless, it was observed an overall decrease in the compressive strength when HA was added to the bulk material, as confirmed by the lowering of the interpolation curve moving from the green data (β-TCP-bulk) to the orange data (HA + β-TCP-bulk).

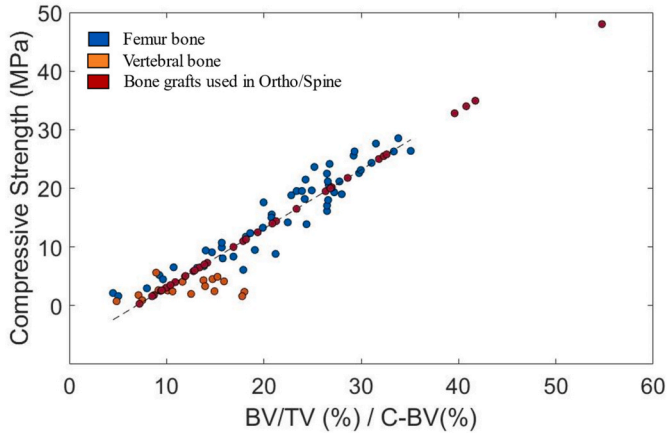

Fig. 5. Compressive strength-BV/TV data for human femur (blue dots) and vertebral bone (orange dots) and compressive strength-C-BV for bone grafts with intended use ortho/spine field (red dots). The human bone data were interpolated through a linear function for the evaluation of C-BV.

3.3.3. Comparison between bone grafts and human bone

Besides the relation between the grafts' porosity with human districts' and between porosity and corresponding mechanical properties, it is possible to perform a deeper morpho-mechanical comparison between human bone and grafts. The value of C-BV was obtained for all the bone grafts presenting values of compressive strength. In Fig. 5 data of femoral and vertebral trabecular bone (in terms of BV/TV and compressive strength) are compared with the same data for the bone grafts which presented as intended use the application in the orthopaedic/spine field. For the femur was observed a BV/TV ranging between 4.5 and 35% corresponding to a compressive strength between 1.6 and 28.6 MPa. Instead, lower values were observed for the trabecular bone of human vertebrae, with a BV/TV ranging from 4.8 to 18% corresponding to a compressive strength from 0.8 to 5.6 MPa. The maximum compressive strength collected for human vertebral bone is almost 80% lower than the maximum value for the femoral trabecular bone.

From literature it was obtained a compressive strength for the grafts used in the ortho/spine field ranging between 0.3 (Collagraft®) and 48 MPa (SuperPore® with 57% of porosity) which corresponds to a C-BV between 7.2 and 55%. Even though Fig. 5 appears to show a superimposition of data related to bone and grafts, almost 74% and 47% of the bone grafts presented a C-BV lower than the mean value of BV/TV for respectively femoral (mean BV/TV = 22%) and vertebral trabecular bone (mean BV/TV = 12%). However, it results that only 4 grafts resulted totally out of the range observed for natural bone with a C-BV of 40.8%, 41.7%, 54.7% and 39.6% for respectively Calcibon®, Osteoset®, SuperPore®-57 and Surgibone®.

4. Discussion

4.1. Different materials and forms, similar intended use

Currently, there is an abundance of commercial bone grafts for the treatment of defects following traumas, tumour resection, etc. This claim is confirmed by the number of scaffolds considered in the present review (n = 62), which represents only a portion of the total commercially available family of devices. The present review sheds light on the most commonly utilized scaffold in the field of bone repair, with load-bearing districts intended use.

Bone grafts vary not only in terms of material composition but also in the supplied form; in several cases, the same material is delivered in a variety of forms based on the need for the specific application. For example, bBONE® is commercially available as blocks, wedges and even granules. The surgeon is free to choose the most suitable form of the same material based on the specific needs, also combining two or more forms for the treatment of the same defect. As for bBONE® most of the here presented grafts are available in different forms.

A lot of these combinations of forms and materials rejoin in the final applications. In fact, for the 82% of the bone substitutes here presented, the manufacturer declared as an indication of use the filling of bone

voids and gaps of the skeletal system or more generally in the orthopaedic surgery field. Instead, almost 34% (some of the scaffolds presented a double indication of use) are intended for oral and/or maxillofacial surgery. All or most of these applications determine, even if in a slight amount, a mechanical solicitation of the implanted scaffold, which needs to withstand this load up to a sufficient osteointegration, which can be achieved from several days to months after implantation, based on the specific properties of the implant.

4.2. Bone grafts require higher mechanical strength in weight-bearing districts

Based on the intended use, the graft should fulfil some mechanical requirements. In particular, when the graft presents a weight-bearing intended use in LBD, as in femur, tibia or spine, it is expected a higher mechanical strength with respect to maxillofacial-application grafts.

A total of 21 grafts presented Oral/CMF application, with a superimposition of intended use with orthopaedic/spine for 10 of them (as stated in the previous paragraph). By excluding these grafts from the following analysis, it is possible to notice that the mean compressive strength for the orthopaedic/spine group is almost 3.3 times higher than the mean value for the Oral/CMF application group (22.4 MPa vs 6.8 MPa). However, great data dispersion is observed with the compressive strength for both the ortho/spine and the oral/CMF groups ranging between 0.31 and 146 MPa and 0.24 and 22.5 MPa, respectively. Anyhow, the graft with higher strength of the latter group (Mimix®) resulted in weaker than 28% of the grafts belonging to the former. This high dispersion should be seen considering that bone grafts, eventually presenting relatively low mechanical strength, are often supported by internal fixation or plating devices meant to provide primary stability and prevent excessive loadings on the bone graft during callus remodelling and maturation phases.

This difference seems to support a substantial difference in the design approach based on the final application: more strength is required for weight-bearing applications, while lower strength is acceptable for oral/CMF use.

4.3. Treatment/sterilization process may affect mechanical properties of allografts

In the present review, 44 out of 62 scaffolds presented a previous study regarding their mechanical characterization. As shown in the results, no available data was found regarding the mechanical and morphological properties of allografts. Even if it could be inferred that there is no need to perform additional material and morphological characterization on bone allografts, as their characteristics are expected to match those of the patient's bone, further considerations must be performed, particularly regarding their sterilization process. Several techniques are adopted by tissue banks to sterilize the explanted bone to be used as an allograft. In particular, three main techniques are reported: chemical procedure, γ-ray irradiation and autoclave. Several studies investigated the effect of all these techniques on the morpho-mechanical properties of trabecular and cortical human bone (Mansor et al., 2023; Costain and Crawford, 2009; Lakhwani et al., 2017). For instance, the Maxgraft® allograft is subjected to a specific certified multi-step process (AlloTec® process) (botiss biomaterials GmbH, 2023) which ends with lyophilization and sterilization via γ-ray irradiation. Even if both Mansor et al. (2023) and Costain et al. (Costain and Crawford, 2009) concluded that for low doses of γ-ray irradiation, no difference is observed in the mechanical response of bone, Lakhwani et al. (2017) determined, instead, a decrease of almost 20% in the compressive strength of bone samples subjected to deep freezing at −76 °C followed by γ-ray irradiation at 25 Gy. So, there is no clear indication of whether the sterilization process via γ-ray can affect the mechanical response of allografts. The lack of available data and the above-mentioned evidence seem to suggest that users should be careful when using allografts, as their final characteristics may be affected by physical factors in different steps of preparation and conservation. Little information is available to date for commercial bone allografts, so efforts to highlight these effects should be encouraged.

4.4. Heterogeneous mechanical testing protocols lead to a lack of comparability

The combination of lack of information and variety in the testing protocols, especially regarding the type of specimen considered (cements rather than blocks or granules) which strongly affect the experimental set-up, leads to difficulty in comparing different bone grafts from a mechanical point of view. Furthermore, no uniformity exists concerning the type of mechanical test performed. As a matter of fact, all the studies presenting graft's mechanical properties performed compression, while only in 5 cases also other loading conditions were considered (i.e. bending, shear and torsion tests).

It is worth to highlight that among 62 bone grafts, only in 6 cases (Alliment®, Cerament®, CortOss®, Osteopal® V, Vertebroplastic® and Bio-Oss®) the scaffold was tested according to standards. In particular, the polymeric-derived grafts (Alliment®, CortOss®, Osteopal® V and Vertebroplastic®) were tested according to the ISO 5833:2002. Instead, Cerament® was tested following the ASTM F2224-09 (2014), which considers high purity Calcium Sulfate Hemihydrate or Dihydrate for surgical implants. Finally, Bio-Oss® was characterised according to the ASTM D695-23 (2023) to compare the results of the mechanical tests with rigid plastic scaffolds.

Of particular interest is to note that even if there exists a standard (ISO 13175-3) for the mechanical characterization of calcium phosphate grafts (ISO 13175-3:2012), none of the considered studies explicitly declare to follow it. This is partially ascribable to the fact that the ISO 13175-3 is not applicable to calcium phosphate cements, which are almost 34% (13 over 38) of the ceramic grafts here considered.

If few standards already exist concerning the mechanical characterization of bone grafts in static conditions, even fewer standards are presently dealing with the characterization in dynamic conditions. As confirmation of this lack of interest, none of the bone grafts except Osteopal® V presented data regarding cyclic tests. In particular, Osteopal® V was tested according to ISO 16402:2008, the only standard dealing with dynamic tests on bone grafts. According to the cited standard, Osteopal® V was tested cyclically in four-point bending to determine the S-N curve (where S is the stress level and N is the number of cycles) and the fatigue strength (runout at $5*10^6$ cycles) (Kö et al., 2013). Besides the above-mentioned ISO, no other standard exists concerning the fatigue tests of bone grafts.

There are some guidelines which could be partially exploited for the dynamic characterization of these devices. In particular, ISO 28704:2011 deals with the cyclic bending fatigue of porous ceramics at room temperature. However, in the 'terms and definition' section it is indicated as porous ceramic a structure with porosity ranging between 30 and 60% (in this work it corresponds to the medium-porosity group) for applications as filters, catalyst carriers etc. but no explicit reference to surgical implants is present.

The above considerations shed light on the need for standards for the static characterization of bone grafts, whatever the form they are delivered (putties, cements etc.). Only through the definition of unique testing protocols, it is possible to properly compare the mechanical properties of different bone grafts. Furthermore, the interest should not focus only on the static mechanical characterizations but also on the fatigue behaviour, due to the fact that the implanted grafts are subjected to cyclic loading conditions up to complete osteointegration.

4.5. Heterogeneous morphological testing protocols lead to a lack of comparability

Similarly to the mechanical properties, the comparison of the

morphological characteristics also presents some issues. Even if porosity seems to be one of the simplest parameters to measure, often it was not reported. Even when this information was supplied, there were discrepancies between different studies. This problem was observed especially regarding bone cement, where the mixing process strongly affects the final structure and as a consequence the morphological properties of the cement (Lewis, 2000; Lindén, 1988). Besides this, the technique exploited to measure morphological properties such as the porosity, leads to differences in the final results. For example, the porosity of Norian® SRS was evaluated in different studies following several techniques. In the study of Luo et al. (2016) two techniques were used to determine the porosity of this bone cement: water evaporation and helium pycnometry. With the former strategy, a porosity of 43.8 ± 1% was determined while a 37.9 ± 0.2% porosity was found for the latter technique. Instead, in the work of Lieshout et al. (Van Lieshout et al., 2011) a total porosity of 0.48 ± 0.15% was determined through micro-CT for the same Norian® SRS cement. Unsurprisingly, this significant difference in porosity did not bring a difference in the final compressive strength between the two studies. In particular, Luo et al. (2016) found a compressive strength equal to 26.5 ± 5.3 MPa while Lieshout et al. (Van Lieshout et al., 2011) a strength of 25.64 ± 7.37 MPa. These results confirm that the difference in porosity between the two studies is merely due to the difference in the technique used to measure it and careful must be paid in considering also the porosities of Eurobone®, HydroSet® and MIIG® X3 which were measured with the same strategy (Van Lieshout et al., 2011). This discrepancy between the porosity evaluated with water immersion and micro-CT was also studied by Yeung et al. (Yeung et al.). They deduced that the disparity in the aforementioned methods derived from a limitation in the micro-CT technique, preventing the assessment of pores smaller than their resolution. In contrast, water immersion encompasses the evaluation of all pores within the structure. This huge variability in the porosity measurement method especially regarding cements is due to a lack of unique standards. Regarding calcium-phosphate scaffolds the ISO 13175-3:2012 deals with the measurement of the graft's porosity. However, this standard is not applicable to calcium phosphate cements, whose value of porosity is mostly affected by the chosen technique. Instead, regarding polymeric-based cement exists the ISO 5833:2002, but no indications regarding the measurement of the porosity are present. Finally, an ISO standard was developed specifically for bone grafts to be used in Oral/Cranio-maxillo-facial applications (ISO 22794:2007) with the limitation of including exclusively devices used for filling and augmenting bone, however excluding grafts made of almost pure hydroxyapatite (>90%). Even if the measure of the porosity is required, the ISO 22794:2007 does not provide any methodology specification.

To obtain reliable measurements of bone grafts' porosity, especially for cements, it is necessary to define a unique method presenting both how to properly prepare the sample and how to test it.

4.6. Significant lack of available data regarding permeability

In recent years, the scaffold's permeability coefficient started to be considered equally to porosity, pore size and interconnectivity as design parameters for porous scaffolds. Its ease of evaluation, with respect to other morphological parameters, makes the permeability coefficient a valid alternative to characterize a scaffold, determining the facility to perfuse and colonize its internal porous structure, allowing nutrients and oxygen to reach the colonizing cells (Pennella et al., 2013). Not only this but in 2014 a standard was published for the measurement of the mean darcy permeability coefficient for a porous scaffold, then revised in 2022 (ASTM F2952-22, 2022).

From the present systematic review appeared clear a significant lack of data regarding the permeability of commercially available scaffolds. In particular, only 15% of the implants (n = 8) were characterized also in terms of permeability and among them 2 were characterized using fluid-dynamics models and the rest through an experimental test-bench exploiting Darcy's law, but none of them explicitly declared to follow a standard for the measurement. This lack of a unique testing protocol for the measurement of the permeability coefficient of porous bone grafts leads to the difficulty in properly comparing the results collected from different studies. The presence of standards should be exploited to have comparable data among different groups.

4.7. Comparison in terms of porosity between scaffold and human bone

Based on the fact that all the presented grafts are intended to be used as bone gaps and void fillers, during working conditions they will interact directly with human bone, mainly trabecular. Thus, it is fundamental that the bone graft matches human natural bone in terms of both mechanical and morphological properties. While the mechanical characteristics are strictly related to several parameters (i.e. bulk material and structural characteristics), the morphology of the bone graft could be partially controlled. It is clear that regarding both allografts and xenografts (except for coral-derived substitutes), the graft's structure is mostly derived from the original bone. As a matter of fact, in the present review, it was found the mean porosity for the xenografts, no matter the intended use, ranging between 69 and 97%, similar to trabecular human bone (Fig. 3).

From Fig. 3 it is interesting to notice that while the grafts used in the Ortho/Spine group presented high variability in terms of porosity, with grafts displaying a significant difference in porosity with respect to natural bone (i.e. CortOss®, Eurobone®, HydroSet®, MIIG® X3 and Osteopla®V), the grafts belonging to the Oral/CMF group presented a much closer porosity with jaw bone. This behaviour is ascribable to the need for compromise between morphology match and mechanical properties for the grafts used in the orthopaedic/spine field, while for the grafts used in the oral/CMF surgery less restrictive requirements are present in terms of mechanical properties, due to lower loads, and more attention could be paid to the graft's morphology. In any case, the observed high variability in porosity should be interpreted positively as well, since it provides a greater selection of bone graft options to accommodate a range of patient situations, from healthy bone to cases of osteoporosis. Furthermore, despite the observed high variability, most of the grafts in the Ortho/spine group belong to the medium/high-porosity group (42% for the high-porosity and 46% for medium-porosity) to resemble as much as possible human natural bone.

To properly resemble human trabecular bone, the grafts should present a porosity possibly in the high range values or at least in the medium one. With low porosity, the colonization from human cells may be affected and slower integration of the bone graft could occur (Lawrence and Madihally, 2008).

4.8. Comparison between bone grafts and human trabecular bone

As presented in paragraph 3.3.3, most of the bone grafts (74%) presented a C-BV lower than the mean BV/TV of the human femoral bone. It means that most bone grafts are typically used as fillers for voids and gaps in the human femur, from a mechanical point of view represents a trabecular bone with too low bone volume fraction with respect to the surrounding tissue. Similarly, 47% of the grafts represent, from a mechanical point of view, a highly porous vertebral trabecular bone, leading to a mismatch between the grafts and the surrounding natural bone structure.

Bone grafts should mimic not only the morphology (as shown in Fig. 3) but also the mechanical properties of natural bone to properly replace native bone during the healing process.

4.9. Limitations of the present work

The present systematic review presents some limitations that must be highlighted:

(i) **Xenografts' origin:** XGs could be derived from different animal species. However, in the present study, only two main species were considered: oxens and corals. In particular, the most numerous group is composed of bone grafts derived from the former species. As a matter of fact, out of 11 XGs here considered (excluding the coral-derived grafts), only two are obtained from animals different from oxen. The employment of animals different from oxen (i.e. horses and pigs) is of rising interest in the last years. However, few devices are still available on the market and even fewer studies on their morpho-mechanical characterization have been found. This is the reason why in the present work, only two xenografts derived from animals different from oxen are presented, which are Osteoplant® obtained from equine bone and Miner-Oss® XP obtained from porcine bone. Other devices have been found, but they presented explicit indications of non-load-bearing district application, therefore they were excluded from the present analysis.

(ii) **Full-text analysis:** As stated in Section 2.2, the full text of each scientific contribution considered has been read by one researcher. By increasing the number of researchers reading the same text, the risk of errors due to misunderstanding or missing data could be reduced.

(iii) **Number of databases:** For the present review only 3 databases have been consulted. Even if they are almost completely exhaustive, still some scientific works may have slipped out.

5. Conclusion

The present work systematically reviews the main bone grafts nowadays available on the market as bone gaps and voids filler in load-bearing districts and sheds light on the lack of data regarding commercially available bone substitutes in terms of morpho-mechanical characteristics. Most of the bone grafts are tested in compression, sometimes according to standards and few of them are tested also in different loading conditions and an even smaller group is characterized also in terms of permeability. The lack of specific standards and test methods does not allow direct data comparability. For these reasons, the comparison between different bone grafts is difficult and it is even harder to define which scaffold is better for a specific intended use.

A complete and transparent morpho-mechanical characterization of commercial bone grafts remains fundamental to support surgeons in the selection of the optimal graft for each intended use and lead to better clinical outcomes, to speed up the research and development of next-generation bone grafts with superior morpho-mechanical characteristics, also taking advantage of predictive digital twins accurately representing the real morphological and mechanical response of the bone grafts in vivo.

CRediT authorship contribution statement

Davide Ninarello: Writing – review & editing, Writing – original draft, Visualization, Methodology, Formal analysis, Data curation, Conceptualization. **Alberto Ballardini:** Writing – review & editing. **Giacomo Morozzi:** Writing – review & editing. **Luigi La Barbera:** Writing – review & editing, Writing – original draft, Visualization, Validation, Supervision, Project administration, Methodology, Investigation, Funding acquisition, Conceptualization.

Declaration of competing interest

The authors declare the following financial interests/personal relationships which may be considered as potential competing interests: Davide Ninarello is supported by NextGenerationEU program, Ministry University and Research, Italia domani – Piano Nazionale di Ripresa e Resilienza.

Giacomo Morozzi and Alberto Ballardini are industry scientists employed by GreenBone Ortho S.p.A (Faenza, Italy) which commercializes one bone grafts (b.BONE™) considered in the present review.

Luigi La Barbera received fundings by GreenBone Ortho S.p.A. for consulting activities outside of the content of the present study.

Acknowledgements

This research work was partially funded by NextGenerationEU program, Italian Ministry of University and Research, Italia domani - Piano Nazionale di Ripresa e Resilienza, Mission 4 "Education & Research", Component C2, CUP D43C23002150008 and GreenBone Ortho S.p.A, Italy.

Data availability

Data will be made available on request.

References

Alt, V., Walter, N., Rupp, M., Begué, T., Plecko, M., 2023. Bone defect filling with a novel rattan-wood based not-sintered hydroxyapatite and beta-tricalcium phosphate material (b.Bone™) after tricortical bone graft harvesting - a consecutive clinical case series of 9 patients. Trauma Case Rep. 44. https://doi.org/10.1016/j.tcr.2023.100805.

Alvis, M., Lalor, P., Brown, M., Morgan, R., Reddi, A., 2000. Successful Induction of New Bone Formation by Callograft, 46th Annual Meeting. Ortopaedic Research Society.

Ammerman, J.M., Libricz, J., Ammerman, M.D., 2013. The role of Osteocel Plus as a fusion substrate in minimally invasive instrumented transforaminal lumbar interbody fusion. Clin. Neurol. Neurosurg. 115 (7), 991–994. https://doi.org/10.1016/j.clineuro.2012.10.013.

ASTM D695-23, 2023. Standard test method for compressive properties of rigid plastics. ASTM International, , 100 Barr Harbor Drive. PO Box C700, West Conshohocken, PA 19428-2959. United States. https://doi.org/10.1520/D0695-23.

ASTM F2224-09, 2014. Standard Specification for High Purity Calcium Sulfate Hemihydrate or Dihydrate for Surgical Implants ASTM International, , 100 Barr Harbor Drive. PO Box C700, West Conshohocken, PA 19428-2959. United States. https://doi.org/10.1520/F2224-09R14.

ASTM F2952-22, 2022. Standard Guide for Determining the Mean Darcy Permeability Coefficient for a Porous Tissue Scaffold, 100 Barr Harbor Drive, PO Box C700. ASTM International, West Conshohocken, PA 19428-2959. United States. https://doi.org/10.1520/F2952-22.

Balakrishnan, M., Agarwal, D.C., Kumar, S., 2000. A study of efficacy of heterogeneous bone grafts (surgibone) in orthopaedic surgery. Med. J. Armed Forces India 56 (1), 21–23. https://doi.org/10.1016/S0377-1237(17)30083-7.

Baskin, J.Z., Vasanji, A., McMasters, J., Soenjaya, Y., Barbu, A.M., Eppell, S.J., 2012. Nanophase bone substitute in vivo response to subcutaneous implantation. J. Biomed. Mater. Res. 100 (9), 2462–2473. https://doi.org/10.1002/jbm.a.34175.

Benefits and associated risks of using allograft, autograft and synthetic bone fusion material for patients and service providers - a Systematic Review. JBI Lib. System. Rev. 8 (8), 2010, 1–13. https://doi.org/10.11124/jbisrir-2010-851.

Berberi, A., Samarani, A., Nader, N., Noujeim, Z., Dagher, M., Kanj, W., Mearawi, R., Salemeh, Z., Badran, B., 2014. Physicochemical characteristics of bone substitutes used in oral surgery in comparison to autogenous bone. BioMed Res. Int. https://doi.org/10.1155/2014/320790.

Bhamb, N., Kanim, L.E.A., Drapeau, S., Mohan, S., Vasquez, E., Shimko, D., McKAY, W., Bae, H.W., 2019. Comparative efficacy of commonly available human bone graft substitutes as tested for posterolateral fusion in an athymic rat model. Internet J. Spine Surg. 13 (5), 437–458. https://doi.org/10.14444/6059.

Bielenstein, J., Radenković, M., Najman, S., Liu, L., Ren, Y., Cai, B., Beuer, F., Rimashevskiy, D., Schnettler, R., Alkildani, S., Jung, O., Schmidt, F., Barbeck, M., 2022. In vivo analysis of the regeneration capacity and immune response to xenogeneic and synthetic bone substitute materials. Int. J. Mol. Sci. 23 (18). https://doi.org/10.3390/ijms231810636.

Bio Coral Calcium Bone, 2019. Universe of Biocoral® [brochure]. Available from: https://biocoral.com/wp-content/uploads/2019/06/Universe-of-Biocoral-VAnglaise-Doc-51-5-17-General.pdf.

Biomaterial, Biovision, 2022a. Bioresorbable bone replacement from microporous and macroporous α-tricalcium phosphate [Brochure]. Available from: https://www.biovision.de/en/products/biobase-ap.

Biomaterial, Biovision, 2022b. Bioresorbable bone replacement from microporous and macroporous α-tricalcium phosphate [Brochure]. Available from: https://www.biovision.de/en/products/biobase.

Biomet, Zimmer, 2018. ProOsteon® bone graft substitute [Brochure]. https://qa-www.zimvie.com/en/spine/biologic-solutions/pro-osteon–bone-graft-substitute.html.

Blokhuis, T.J., 2014. Bioresorbable bone graft substitutes. In: Mallick, K. (Ed.), Bone Substitute Biomaterials. Woodhead Publishing, pp. 80–92.

Blom, A.W., Cunningham, J.L., Hughes, G., Lawes, T.J., Smith, N., Blunn, G., Learmonth, I.D., Goodship, A.E., 2005. The compatibility of ceramic bone graft substitutes as allograft extenders for use in impaction grafting of the femur. J. Bone Joint Surg. Br. 87 (3), 421–425. https://doi.org/10.1302/0301-620x.87b3.14337.

Blom, A.W., Wylde, V., Livesey, C., Whitehouse, M.R., Eastaugh-Waring, S., Bannister, G. C., Learmonth, I.D., 2009. Impaction bone grafting of the acetabulum at hip revision using a mix of bone chips and a biphasic porous ceramic bone graft substitute. Acta Orthop. 80 (2), 150–154. https://doi.org/10.3109/17453670902884767.

Boffa, A., Solaro, L., Poggi, A., Andriolo, L., Reale, D., Di Martino, A., 2021. Multi-layer cell-free scaffolds for osteochondral defects of the knee: a systematic review and meta-analysis of clinical evidence. J. Exp. Orthop. 8 (1). https://doi.org/10.1186/s40634-021-00377-4.

Botez, P., Sirbu, P., Simion, L., et al., 2009. Application of a biphasic macroporous synthetic bone substitutes CERAFORM®: clinical and histological results. Eur. J. Orthop. Surg. Traumatol. 19, 387–395. https://doi.org/10.1007/s00590-009-0445-7.

botiss biomaterials GmbH, maxresorb® & maxresorb® inject INNOVATIVE BIPHASIC CALCIUM PHOSPHATE [Brochure]. https://www.botiss.com/pdf/botiss_maxresorb_EN.pdf.

botiss biomaterials GmbH, 2023. maxgraft® cortico maxgraft® bonebuilder maxgraft® bonering PROCESSED HUMAN ALLOGRAFT [Brochure]. Available from: https://www.botiss.com/pdf/botiss_maxgraft_EN.pdf.

Brueckner, T., Heilig, P., Jordan, M.C., Paul, M.M., Blunk, T., Meffert, R.H., Gbureck, U., Hoelscher-Doht, S., 2019a. Biomechanical evaluation of promising different bone substitutes in a clinically relevant test set-up. Materials 12 (9). https://doi.org/10.3390/ma12091364.

Brueckner, T., Heilig, P., Jordan, M.C., Paul, M.M., Blunk, T., Meffert, R.H., Gbureck, U., Hoelscher-Doht, S., 2019b. Biomechanical evaluation of promising different bone substitutes in a clinically relevant test set-up. Materials 12. https://doi.org/10.3390/ma12091364.

Cabbar, F., Güler, N., Kürkcü, M., Işeri, U., Sençift, K., 2011. The effect of bovine bone graft with or without platelet-rich plasma on maxillary sinus floor augmentation. J. Oral Maxillofac. Surg. 69 (10), 2537–2547. https://doi.org/10.1016/j.joms.2011.03.040.

Cendre, E., Mitton, D., Roux, J.P., Arlot, M.E., Duboeuf, F., Burt-Pichat, B., Rumelhart, C., Peix, G., Meunier, P.J., 1999a. High-resolution computed tomography for architectural characterization of human lumbar cancellous bone: relationships with histomorphometry and biomechanics. Osteoporos. Int. 10 (5), 353–360. https://doi.org/10.1007/s001980050240.

Cendre, E., Mitton, D., Roux, J.P., Arlot, M.E., Duboeuf, F., Burt-Pichat, B., Rumelhart, C., Peix, G., Meunier, P.J., 1999b. High-resolution computed tomography for architectural characterization of human lumbar cancellous bone: relationships with histomorphometry and biomechanics. Osteoporos. Int. 10 (5), 353–360. https://doi.org/10.1007/s001980050240.

Chang, L.C., 2021. Comparison of clinical parameters in dental implant therapy between implant site development using porcine- and bovine-derived xenografts. Technologies 9 (72). https://doi.org/10.3390/technologies9040072.

Changoor, A., Hurtig, M.B., John Runciman, R., 2006. Osteochondral graft fixation using a bioresorbable bone cement. J. Biomech. 39 (15), 2887–2892. https://doi.org/10.1016/j.jbiomech.2005.10.007.

Chen, C.L., Liu, C.L., Sun, S.S., Han, P.Y., Lee, C.S., Lo, W.H., 2006. Posterolateral lumbar spinal fusion with autogenous bone chips from laminectomy extended with OsteoSet. J. Chin. Med. Assoc. 69 (12), 581–584. https://doi.org/10.1016/s1726-4901(09)70333-8.

Chen, C.-H., Chiang, C.-J., Rau, G., Huang, M.-S., Chan, K.K., Liao, C.-J., Kuo, Y.-J., 2012. In vivo evaluation of a new biphasic calcium phosphate bone substitute in rabbit femur defects model. Biomed. Eng. Appl. Basis Commun. 24 (6), 537–548.

Chen, Y.J., Pao, J.L., Chen, C.S., Chen, Y.C., Chang, C.C., Hung, F.M., Chang, C.H., 2017. Evaluation of new biphasic calcium phosphate bone substitute: rabbit femur defect model and preliminary clinical results. J. Med. Biol. Eng. 37 (1), 85–93. https://doi.org/10.1007/s40846-016-0203-3.

Chiarello, E., Cadossi, M., Tedesco, G., Capra, P., Calamelli, C., Shehu, A., Giannini, S., 2013. Autograft, allograft and bone substitutes in reconstructive orthopedic surgery. Aging Clin. Exp. Res. 25 (Suppl. 1), 101–103. https://doi.org/10.1007/s40520-013-0088-8.

Clarkin, O.M., Boyd, D., Madigan, S., Towler, M.R., 2009. Comparison of an experimental bone cement with a commercial control, Hydroset. J. Mater. Sci. Mater. Med. 20 (7), 1563–1570. https://doi.org/10.1007/s10856-009-3701-9.

Cornell, C.N., Lane, J.M., Chapman, M., Merkow, R., Seligson, D., Henry, S., Gustilo, R., Vincent, K., 1991. Multicenter trial of Collagraft as bone graft substitute. J. Orthop. Trauma 5 (1), 1–8.

Costain, D.J., Crawford, R.W., 2009. Fresh-frozen vs. irradiated allograft bone in orthopaedic reconstructive surgery. Injury 40 (12), 1260–1264. https://doi.org/10.1016/j.injury.2009.01.116.

Cottrill, E., Pennington, Z., Wolf, M.T., Dirckx, N., Ehresman, J., Perdomo-Pantoja, A., Rajkovic, C., Lin, J., Maestas, D.R., Mageau, A., Lambrechts, D., Stewart, V., Sciubba, D.M., Theodore, N., Elisseeff, J.H., Witham, T., 2023. Creation and preclinical evaluation of a novel mussel-inspired, biomimetic, bioactive bone graft scaffold: direct comparison with Infuse bone graft using a rat model of spinal fusion. J. Neurosurg. Spine 39 (1), 113–121. https://doi.org/10.3171/2023.2.SPINE22936.

Coulson, R., Clokie, C.M.L., Peel, S., 1999. Collagen and a Thermally Reversible Poloxamer Deliver Demineralized Bone Matrix (DBM) and Biologically Active Proteins to Sites of Bone Regeneration.

Cunha, C., Sprio, S., Panseri, S., Dapporto, M., Marcacci, M., Tampieri, A., 2013. High biocompatibility and improved osteogenic potential of novel Ca-P/titania composite scaffolds designed for regeneration of load-bearing segmental bone defects. J. Biomed. Mater. Res. 101 (6), 1612–1619. https://doi.org/10.1002/jbm.a.34479.

D'Alessandro, D., Perale, G., Milazzo, M., Moscato, S., Stefanini, C., Pertici, G., Danti, S., 2017. Bovine bone matrix/poly(l-lactic-co-ε-caprolactone)/gelatin hybrid scaffold (SmartBone®) for maxillary sinus augmentation: a histologic study on bone regeneration. Int. J. Pharm. 523 (2), 534–544. https://doi.org/10.1016/j.ijpharm.2016.10.036.

Daculsi, G., LeGeros, R., 2008. Tricalcium phosphate/hydroxyapatite biphasic ceramics. In: Kokubo, T. (Ed.), Bioceramics and Their Clinical Applications, first ed. Woodhead Publishing, Chubu, pp. 395–416. https://doi.org/10.1533/9781845694227.2.395.

Daculsi, G., Fellah, B., Miramond, T., Durand, M., Osteoconduction, Osteogenicity, 2013. Osteoinduction, what are the fundamental properties for a smart bone substitutes. IRBM 34, 346–348. https://doi.org/10.1016/j.irbm.2013.07.001.

Dadkhah, M., Pontiroli, L., Fiorilli, S., Manca, A., Tallia, F., Tcacencu, I., Vitale-Brovarone, C., 2016. Preparation and characterization of an innovative injectable calcium sulphate based bone cement for vertebroplasty application. J. Mater. Chem. B 5. https://doi.org/10.1039/C6TB02139E.

Decambron, A., Manassero, M., Bensidhoum, M., Lecuelle, B., Logeart-Avramoglou, D., Petite, H., Viateau, V., 2017. A comparative study of tissue-engineered constructs from Acropora and Porites coral in a large animal bone defect model. Bone Joint Res. 6 (4), 208–215. https://doi.org/10.1302/2046-3758.64.BJR-2016-0236.R1.

Demers, C., Hamdy, C.R., Corsi, K., Chellat, F., Tabrizian, M., Yahia, L., 2002. Natural coral exoskeleton as a bone graft substitute: a review. Bio Med. Mater. Eng. 12 (1), 15–35.

Dempster, D.W., Ferguson-Pell, M.W., Mellish, R.W., Cochran, G.V., Xie, F., Fey, C., Horbert, W., Parisien, M., Lindsay, R., 1993. Relationships between bone structure in the iliac crest and bone structure and strength in the lumbar spine. Osteoporos. Int. 3 (2), 90–96. https://doi.org/10.1007/BF01623379.

DePuy Spine, Spine, 2023. UNIPLATE® anterior cervical plate system [brochure]. Available from: https://thespinemarketgroup.com/wp-content/uploads/2023/02/Uniplate-SGT.DepuySynthes.pdf.

DiCicco, M., Duong, T., Chu, A., Jansen, S.A., 2003. Tobramycin and gentamycin elution analysis between two in situ polymerizable orthopedic composites. J. Biomed. Mater. Res. B Appl. Biomater. 65 (1), 137–149. https://doi.org/10.1002/jbm.b.10528.

Ding, M., Dalstra, M., Danielsen, C.C., Kabel, J., Hvid, I., Linde, F., 1997a. Age variations in the properties of human tibial trabecular bone. J. Bone Joint Surg. Br. 79 (6), 995–1002. https://doi.org/10.1302/0301-620x.79b6.7538.

Ding, M., Dalstra, M., Danielsen, C.C., Kabel, J., Hvid, I., Linde, F., 1997b. Age variations in the properties of human tibial trabecular bone. J. Bone Joint Surg. Br. 79 (6), 995–1002. https://doi.org/10.1302/0301-620x.79b6.7538.

Dinopoulos, H.T., Giannoudis, P.V., 2006. Safety and efficacy of use of demineralised bone matrix in orthopaedic and trauma surgery. Expet Opin. Drug Saf. 5 (6), 847–866. https://doi.org/10.1517/14740338.5.6.847.

Dorati, R., Colonna, C., Genta, I., Bruni, G., Visai, L., Conti, B., 2014. Preparation and characterization of an advanced medical device for bone regeneration. AAPS PharmSciTech 15 (1), 75–82. https://doi.org/10.1208/s12249-013-0033-3.

Duncan, S.T., Sabatini, F., 2023. The use of calcium sulfate/hydroxyapatite bone graft substitute to restore acetabular bone loss in revision total hip arthroplasty. Arthroplast Today 23. https://doi.org/10.1016/j.artd.2023.101217.

Euroteknika, Macrobone [Brochure]. https://www.dental-leader.it/Schede_prodotti/Schede_tecniche/Scheda_tecnica_22-508.pdf.

Falvo D'Urso Labate, G., Baino, F., Terzini, M., Audenino, A., Vitale-Brovarone, C., Segers, P., Quarto, R., Catapano, G., 2016. Bone structural similarity score: a multiparametric tool to match properties of biomimetic bone substitutes with their target tissues. J. Appl. Biomater. Funct. Mater. 14 (3), 277–289. https://doi.org/10.5301/jabfm.5000283.

Farrar, N., 2015. Short Term Release and Mechanical Strength of Fluorescein-Impregnated Calcium Sulfate Beads. The Ohio State University.

Fassina, L., Saino, E., De Angelis, M.G., Magenes, G., Benazzo, F., Visai, L., 2010. Low-power ultrasounds as a tool to culture human osteoblasts inside cancellous hydroxyapatite. Bioinorgan. Chem. Appl. https://doi.org/10.1155/2010/456240.

Feng, F., Chen, M., Wang, X., Zhang, H., Nie, H., Tang, H., 2021. Translation of a spinal bone cement product from bench to bedside. Bioact. Mater. 10, 345–354. https://doi.org/10.1016/j.bioactmat.2021.08.011.

Fin-Ceramica Faenza S.p.A., Pre-Formed Bone Substitute Engineered for orthopaedic surgery [Brochure]. https://www.finceramica.it/wps/wcm/connect/internet/af0fe62f-74a8-4141-84f1-d1f1d88ff6d8/MDU009000-09-00+Brochure+ENGIpore+OrthoSpine+IT+2018+LOW.pdf?MOD=AJPERES&CONVERT_TO=url&CACHEID=ROOTWORKSPACE.Z18_M1H4H9O0PGD000QM03CV7O0002-af0fe62f-74a8-4141-84f1-d1f1d88ff6d8-nVoJ7PS.

Follet, H., Viguet-Carrin, S., Burt-Pichat, B., Dépalle, B., Bala, Y., Gineyts, E., Munoz, F., Arlot, M., Boivin, G., Chapurlat, R.D., Delmas, P.D., Bouxsein, M.L., 2011a. Effects of preexisting microdamage, collagen cross-links, degree of mineralization, age, and architecture on compressive mechanical properties of elderly human vertebral trabecular bone. J. Orthop. Res. 29 (4), 481–488. https://doi.org/10.1002/jor.21275.

Follet, H., Viguet-Carrin, S., Burt-Pichat, B., Dépalle, B., Bala, Y., Gineyts, E., Munoz, F., Arlot, M., Boivin, G., Chapurlat, R.D., Delmas, P.D., Bouxsein, M.L., 2011b. Effects of preexisting microdamage, collagen cross-links, degree of mineralization, age, and architecture on compressive mechanical properties of elderly human vertebral trabecular bone. J. Orthop. Res. 29 (4), 481–488. https://doi.org/10.1002/jor.21275.

Frayssinet, P., Roudier, M., Lerch, A., Ceolin, J.L., Deprès, E., Rouquet, N., 2000. Tissue reaction against a self-setting calcium phosphate cement set in bone or outside the organism. J. Mater. Sci. Mater. Med. 11 (12), 811–815. https://doi.org/10.1023/a:1008909714090.

Friesenbichler, J., Maurer-Ertl, W., Bergovec, M., Holzer, L.A., Ogris, K., Leitner, L., Leithner, A., 2017. Clinical experience with the artificial bone graft substitute

Calcibon used following curettage of benign and low-grade malignant bone tumours. Sci. Rep. 7 (1). https://doi.org/10.1038/s41598-017-02048-w.
Fyhrie, D.P., Lang, S.M., Hoshaw, S.J., Schaffler, M.B., Kuo, R.F., 1995. Human vertebral cancellous bone surface distribution. Bone 17 (3), 287–291. https://doi.org/10.1016/8756-3282(95)00218-3.
Gagala, J., 2021. Minimum 10 years clinical and radiological outcomes of acetabular revisions of total hip arthroplasties with tricalcium phosphate/hydroxyapatite bone graft substitute. BMC Muscoskel. Disord. 22 (1). https://doi.org/10.1186/s12891-021-04694-8.
Galois, L., Mainard, D., Delagoutte, J.P., 2002. Beta-tricalcium phosphate ceramic as a bone substitute in orthopaedic surgery. Int. Orthop. 26 (2), 109–115. https://doi.org/10.1007/s00264-001-0329-x.
Galovich, L.A., Perez-Higueras, A., Altonaga, J.R., Orden, J.M., Barba, M.L., Morillo, M. T., 2011. Biomechanical, histological and histomorphometric analyses of calcium phosphate cement compared to PMMA for vertebral augmentation in a validated animal model. Eur. Spine J. 20 (Suppl. 3), 376–382. https://doi.org/10.1007/s00586-011-1905-4.
Geistlich Pharma, A.G., 2005. Orthoss Orthoss® collagen [brochure]. Available from: https://www.geistlich-pharma.com/fileadmin/content/International_Pharma/PDF/Orthopedic/Bro_Orthoss_Orthoss_Collagen_EN.pdf.
Gheduzzi, S., Webb, J.J., Miles, A.W., 2006. Mechanical characterisation of three percutaneous vertebroplasty biomaterials. J. Mater. Sci. Mater. Med. 17 (5), 421–426. https://doi.org/10.1007/s10856-006-8469-6.
Giesen, E.B., van Eijden, T.M., 2000. The three-dimensional cancellous bone architecture of the human mandibular condyle. J. Dent. Res. 79 (4), 957–963. https://doi.org/10.1177/00220345000790041101.
Giuliani, A., Manescu, A., Larsson, E., Tromba, G., Luongo, G., Piattelli, A., Mangano, F., Iezzi, G., Mangano, C., 2014. In vivo regenerative properties of coralline-derived (biocoral) scaffold grafts in human maxillary defects: demonstrative and comparative study with Beta-tricalcium phosphate and biphasic calcium phosphate by synchrotron radiation x-ray microtomography. Clin. Implant Dent. Relat. Res. 16 (5), 736–750. https://doi.org/10.1111/cid.12039.
Goebel, J.A., Jacob, A., 2005. Use of Mimix hydroxyapatite bone cement for difficult ossicular reconstruction. Otolaryngol. Head Neck Surg. 132 (5), 727–734. https://doi.org/10.1016/j.otohns.2005.01.023.
Gordon, D.T., 2005. Effects of Biochemical and Mechanical Stimulation of Articular Chondrocytes in Collagen-Gag Scaffolds: Extracellular Matrix Biosynthesis and Scaffold Stiffness. Massachusetts Institute of Technology, Massachusetts.
Granville, M., Jacobson, R.E., 2017. An innovative use of cortoss bone cement to stabilize a nonunion after interbody fusion. Cureus 9 (1). https://doi.org/10.7759/cureus.986.
Greenbone Ortho, S.p.A., 2023. GreenBone® NATURAL BONE HEALING [brochure]. Available from: https://greenbone.it/publication/product-catalogue.
Greenspan, D.C., 2013. Comparison of A synthetic and bovine derived hydroxyapatite bone graft substitute. Zimmer Dental. Inc.
Grottoli, C.F., Cingolani, A., Zambon, F., Ferracini, R., Villa, T., Perale, G., 2019. Simulated performance of a xenohybrid bone graft (SmartBone®) in the treatment of acetabular prosthetic reconstruction. J. Funct. Biomater. 10 (4). https://doi.org/10.3390/jfb10040053.
Guarnieri, G., Vassallo, P., Muto, M., Muto, M., 2013. Percutaneous treatment of symptomatic aneurysmal bone cyst of L5 by percutaneous injection of osteoconductive material (Cerament). BMJ Case Rep. https://doi.org/10.1136/bcr-2013-010912.
Haddock, S.M., Debes, J.C., Nauman, E.A., Fong, K.E., Arramon, Y.P., Keaveny, T.M., 1999. Structure-function relationships for coralline hydroxyapatite bone substitute. J. Biomed. Mater. Res. 47 (1), 71–78. https://doi.org/10.1002/(sici)1097-4636(199910)47:1<71::aid-jbm10>3.0.co;2-u.
Haenle, M., Schlüter, S., Ellenrieder, M., Mittelmeier, W., Bader, R., 2013. Treatment of acetabular defects during revision total hip arthroplasty–preliminary clinical and radiological outcome using bone substitute materials. Hip Int. 23 (1), 46–53. https://doi.org/10.5301/HIP.2013.10713.
Handal, J.A., Schulz, J.F., Pahys, J.M., Williams, E.A., Kwok, S.C., Samuel, S.P., 2011. Evaluation of elution and mechanical properties of two injectable chemotherapeutic bone cements. Chemotherapy 57 (3), 268–274. https://doi.org/10.1159/000327388.
Hannink, G., Wolke, J.G., Schreurs, B.W., Buma, P., 2008. In vivo behavior of a novel injectable calcium phosphate cement compared with two other commercially available calcium phosphate cements. J. Biomed. Mater. Res. B Appl. Biomater. 85 (2), 478–488.
He, Z., Zhai, Q., Hu, M., Cao, C., Wang, J., Yang, H., Li, B., 2014. Bone cements for percutaneous vertebroplasty and balloon kyphoplasty: current status and future developments. J. Orthop. Translat. 3 (1), 1–11. https://doi.org/10.1016/j.jot.2014.11.002.
Heini, P.F., Berlemann, U., 2001. Bone substitutes in vertebraplasty. Eur. Spine J. 10 (Suppl. 2), 205–213. https://doi.org/10.1007/s005860100308.
Heraeus, 2008. Materiale per rigenerazione ossea nanocristallino Ready to use [Brochure]. https://www.territo.it/UserFiles/File/Products/6631_Ostim_Brochure_IT.pdf.
Heraeus Medical GmbH (2020), Osteopal® V Radiopaque bone cement for filling and stabilising vertebral bodies [Brochure]. https://www.heraeus.com/media/media/hme/doc_hme/products_us/OSTEOPAL_V_IFU.pdf.
Hess, T., Gleitz, M., Hanser, U., Mittelmeier, H., Kubale, R., 1995. Die primäre Belastbarkeit autologer und heterologer Implantate für die interkorporelle Spondylodese. Z. Orthop. Ihre Grenzgeb. 133 (3), 222–226. https://doi.org/10.1055/s-2008-1039441.
Hing, K., 2005. Bioceramic bone graft substitutes: influence of porosity and chemistry. Int. J. Appl. Ceram. Technol. 2, 184–199. https://doi.org/10.1111/j.1744-7402.2005.02020.x.
Hing, K.A., Best, S.M., Bonfield, W., 1999. Characterization of porous hydroxyapatite. J. Mater. Sci. Mater. Med. 10, 135–145. https://doi.org/10.1023/A:1008929305897.
Huber, F.X., Berger, I., McArthur, N., Huber, C., Kock, H.P., Hillmeier, J., Meeder, P.J., 2008. Evaluation of a novel nanocrystalline hydroxyapatite paste and a solid hydroxyapatite ceramic for the treatment of critical size bone defects (CSD) in rabbits. J. Mater. Sci. Mater. Med. 19 (1), 33–38. https://doi.org/10.1007/s10856-007-3039-0.
IBI SA, 2015. Smartbone® [brochure]. Available from: https://puredent.dk/pdf/techInfos20Smartbone.pdf.
Ikuta, K., Nishida, Y., Ota, T., et al., 2022. A clinical trial of a unidirectional porous tricalcium phosphate filling for defects after resection of benign bone lesions: a prospective multicenter study. Sci. Rep. 12. https://doi.org/10.1038/s41598-022-20359-5.
Institut Straumann AG, 2017. Botiss cerabone® MATERIALE DA INNESTO DI OSSO BOVINO NATURALE [Brochure]. Available from: https://www.straumann.com/content/dam/media-center/straumann/it/documents/brochure/product-information/490.353-it_low.pdf.
International Organization for StandardizationAcrylic resin. Implants for surgery — Acrylic resin cements (ISO Standard No. 5833:2002). https://www.iso.org/standard/30980.html.
International Organization for Standardization Calcium phosphates. Implants for surgery — Calcium phosphates — Part 3: Hydroxyapatite and beta-tricalcium phosphate bone substitutes (ISO Standard No. 13175-3:2012). https://www.iso.org/standard/53447.html.
International Organization for Standardization Implants for surgery. Implants for surgery Acrylic resin cement Flexural fatigue testing of acrylic resin cements used in orthopaedics (ISO Standard No. 16402:2008). https://www.iso.org/standard/32212.html.
International Organization for Standardization Fine ceramics. Fine ceramics (advanced ceramics, advanced technical ceramics): Test method for cyclic bending fatigue of porous ceramics at room temperature. (ISO Standard No. 28704:2011). https://www.iso.org/standard/53008.html.
International Organization for Standardization Dentistry. Dentistry - Implantable materials for bone filling and augmentation in oral and maxillofacial surgery — Contents of a technical file (ISO Standard No. 22794:2007). https://www.iso.org/standard/40138.html.
Iundusi, R., Gasbarra, E., D'Arienzo, M., Piccioli, A., Tarantino, U., 2015. Augmentation of tibial plateau fractures with an injectable bone substitute: CERAMENT™. Three year follow-up from a prospective study. BMC Muscoskel. Disord. 13. https://doi.org/10.1186/s12891-015-0574-6.
Jensen, T., Schou, S., Stavropoulos, A., Terheyden, H., Holmstrup, P., 2012. Maxillary sinus floor augmentation with Bio-Oss or Bio-Oss mixed with autogenous bone as graft in animals: a systematic review. Int. J. Oral Maxillofac. Surg. 41 (1), 114–120. https://doi.org/10.1016/j.ijom.2011.08.010.
Joeris, A., Ondrus, S., Planka, L., Gal, P., Slongo, T., 2010. ChronOS inject in children with benign bone lesions–does it increase the healing rate? Eur. J. Pediatr. Surg. 20 (1), 24–28. https://doi.org/10.1055/s-0029-1241866.
Kallala, R., Harris, W.E., Ibrahim, M., Dipane, M., McPherson, E., 2018a. Use of Stimulan absorbable calcium sulphate beads in revision lower limb arthroplasty: safety profile and complication rates. Bone Joint Res. 7 (10), 570–579. https://doi.org/10.1302/2046-3758.710.BJR-2017-0319.R1. PMID: 30464837; PMCID: PMC6215242.
Kallala, R., Harris, W.E., Ibrahim, M., Dipane, M., McPherson, E., 2018b. Use of Stimulan absorbable calcium sulphate beads in revision lower limb arthroplasty: safety profile and complication rates. Bone Joint Res. 7 (10), 570–579. https://doi.org/10.1302/2046-3758.710.BJR-2017-0319.R1.
Kayal, C., Ozan, F., Altay, T., Karahan, H.G., Yamak, K., Özdemir, S., 2021. Efficacy of calcium phosphate cementing in the surgical treatment of Sanders Type II and III calcaneal fractures using screw fixation with sinus tarsi approach. Acta Orthop. Traumatol. Turcica 55 (3), 265–270. https://doi.org/10.5152/j.aott.2021.20188.
Kim, J.E., Shin, J.M., Oh, S.O., Yi, W.J., Heo, M.S., Lee, S.S., Choi, S.C., Huh, K.H., 2013. The three-dimensional microstructure of trabecular bone: analysis of site-specific variation in the human jaw bone. Imaging Sci. Dent. 43 (4), 227–233. https://doi.org/10.5624/isd.2013.43.4.227.
Kloss, F.R., Kämmerer, P.W., Kloss-Brandstätter, A., 2023. First clinical case report of a xenograft-allograft combination for alveolar ridge augmentation using a bovine bone substitute material with hyaluronate (Cerabone® plus) combined with allogeneic bone granules (Maxgraft®). J. Clin. Med. 12 (19). https://doi.org/10.3390/jcm12196214.
Köster, U., Jaeger, R., Bardts, M., Wahnes, C., Büchner, H., Kühn, K.D., Vogt, S., 2013. Creep and fatigue behavior of a novel 2-component paste-like formulation of acrylic bone cements. J. Mater. Sci. Mater. Med. 24 (6), 1395–1406. https://doi.org/10.1007/s10856-013-4909-2.
Kon, E., Salamanna, F., Filardo, G., Di Matteo, B., Shabshin, N., Shani, J., Fini, M., Perdisa, F., Parrilli, A., Sprio, S., Ruffini, A., Marcacci, M., Tampieri, A., 2021. Bone regeneration in load-bearing segmental defects, guided by biomorphic, hierarchically structured apatitic scaffold. Front. Bioeng. Biotechnol. 9. https://doi.org/10.3389/fbioe.2021.734486.
Kondo, N., Ogose, A., Tokunaga, K., Umezu, H., Arai, K., Kudo, N., Hoshino, M., Inoue, H., Irie, H., Kuroda, K., Mera, H., Endo, N., 2006. Osteoinduction with highly purified beta-tricalcium phosphate in dog dorsal muscles and the proliferation of osteoclasts before heterotopic bone formation. Biomaterials 27 (5), 4419–4427. https://doi.org/10.1016/j.biomaterials.2006.04.016.

Krennmair, S., Postl, L., Schwarze, U.Y., Malek, M., Stimmelmayr, M., Krennmair, G., 2023. Clinical, radiographic, and histological/histomorphometric analysis of maxillary sinus grafting with deproteinized porcine or bovine bone mineral: a randomized clinical trial. Clin. Oral Implants Res. 34 (11), 1230–1247. https://doi.org/10.1111/clr.14164.

Kübler, A., Neugebauer, J., Oh, J.H., Scheer, M., Zöller, J.E., 2004. Growth and proliferation of human osteoblasts on different bone graft substitutes: an in vitro study. Implant Dent. 13 (2), 171–179. https://doi.org/10.1097/01.id.0000127522.14067.11.

Kuemmerle, J.M., Oberle, A., Oechslin, C., Bohner, M., Frei, C., Boecken, I., von Rechenberg, B., 2005. Assessment of the suitability of a new brushite calcium phosphate cement for cranioplasty - an experimental study in sheep. J. Cranio-Maxillo-Fac. Surg. 33 (1), 37–44. https://doi.org/10.1016/j.jcms.2004.09.002.

Kurashina, K., Kurita, H., Hirano, M., De Blieck, J.M.A., Klein, C.P.A.T., De Groot, K., 1995. Calcium phosphate cement: in vitro and in vivo studies of the α-tricalcium phosphate-dicalcium phosphate dibasic-tetracalcium phosphate monoxide system. J. Mater. Sci. Mater. Med. 6, 340–347.

Kurien, T., Pearson, R.G., Scammell, B.E., 2013. Bone graft substitutes currently available in orthopaedic practice: the evidence for their use. Bone Joint Lett. J 95-B (5), 583–597. https://doi.org/10.1302/0301-620X.95B5.30286.

Lakhwani, O.P., Jindal, M., Kaur, O., Chandoke, R.K., Kapoor, S.K., 2017. Effect of bone bank processing on bone mineral density, histomorphometry & biomechanical strength of retrieved femoral head. Indian J. Med. Res. 146 (Suppl. l), 45–50. https://doi.org/10.4103/ijmr.IJMR_739_15.

Lancianese, S.L., Kwok, E., Beck, C.A., Lerner, A.L., 2008. Predicting regional variations in trabecular bone mechanical properties within the human proximal tibia using MR imaging. Bone 43 (6), 1039–1046. https://doi.org/10.1016/j.bone.2008.07.247.

Lauritano, D., Carinci, F., Zollino, I., Hassanipour, A., Saggese, V., Palmieri, A., Girardi, A., Cura, F., Piras, A., Zamboni, P., Brunelli, G., 2012. Osteoplant acts on stem cells derived from bone marrow inducing osteoblasts differentiation. Eur. J. Inflamm. 10, 89–94.

Lawrence, B.J., Madihally, S.V., 2008. Cell colonization in degradable 3D porous matrices. Cell Adhes. Migrat. 2 (1), 9–16. https://doi.org/10.4161/cam.2.1.5884.

Le Ferrec, M., Mellier, C., Lefèvre, F.X., Boukhechba, F., Janvier, P., Montavon, G., Bouler, J.M., Gauthier, O., Bujoli, B., 2020. In vivo resorption of injectable apatitic calcium phosphate cements: critical role of the intergranular microstructure. J. Biomed. Mater. Res. B Appl. Biomater. 108 (2), 367–376. https://doi.org/10.1002/jbm.b.34395.

Lee, S.J., Lim, G.J., Lee, J.W., Atala, A., Yoo, J.J., 2006. In vitro evaluation of a poly (lactide-co-glycolide)-collagen composite scaffold for bone regeneration. Biomaterials 27 (18), 3466–3472. https://doi.org/10.1016/j.biomaterials.2006.01.059.

Leupold, J.A., Barfield, W.R., An, Y.H., Hartsock, L.A., 2006. A comparison of ProOsteon, DBX, and collagraft in a rabbit model. J. Biomed. Mater. Res. B Appl. Biomater. 79 (2), 292–297. https://doi.org/10.1002/jbm.b.30541.

Lewis, G., 2000. Relative roles of cement molecular weight and mixing method on the fatigue performance of acrylic bone cement: simplex P versus Osteopal. J. Biomed. Mater. Res. 53 (1), 119–130. https://doi.org/10.1002/(sici)1097-4636(2000)53:1<119::aid-jbm16>3.0.co;2-n.

Li, S., De Wijn, J.R., Li, J., Layrolle, P., De Groot, K., 2003. Macroporous biphasic calcium phosphate scaffold with high permeability/porosity ratio. Tissue Eng. 9 (3), 535–548. https://doi.org/10.1089/107632703322066714.

Lindén, U., 1988. Porosity in manually mixed bone cement. Clin. Orthop. Relat. Res. 231, 110–112.

Lorenz, J., Schlee, M., Al-Maawi, S., Chia, P., Sader, R.A., Ghanaati, S., 2017. Variant purification of an allogeneic bone block. Acta Stomatol. Croat. 51 (2), 141–147. https://doi.org/10.15644/asc51/2/7.

Luo, J., Ajaxon, I., Ginebra, M.P., Engqvist, H., Persson, C., 2016. Compressive, diametral tensile and biaxial flexural strength of cutting-edge calcium phosphate cements. J. Mech. Behav. Biomed. Mater. 60, 617–627. https://doi.org/10.1016/j.jmbbm.2016.03.028.

Mai, R., Reinstorf, A., Pilling, E., Hlawitschka, M., Jung, R., Gelinsky, M., Schneider, M., Loukota, R., Pompe, W., Eckelt, U., Stadlinger, B., 2008. Histologic study of incorporation and resorption of a bone cement-collagen composite: an in vivo study in the minipig. Oral Surg. Oral Med. Oral Pathol. Oral Radiol. Endod. 105 (3), 9–14. https://doi.org/10.1016/j.tripleo.2007.09.016.

Mallick, M., Are, R., Babu, A., 2022. An overview of collagen/bioceramic and synthetic collagen for bone tissue engineering. Materialia 22. https://doi.org/10.1016/j.mtla.2022.101391.

Mann, R.J., Blount, A.L., Neaman, K.C., Korepta, L., 2011. Mimix hydroxyapatite cement use in the reconstruction of the craniofacial skeleton. J. Craniofac. Surg. 22 (6), 2144–2147. https://doi.org/10.1097/SCS.0b013e3182323ca8.

Mansor, A., Ariffin, A.F., Yusof, N., Mohd, S., Ramalingam, S., Md Saad, A.P., Baharin, R., Min, N.W., 2023. Effects of processing and gamma radiation on mechanical properties and organic composition of frozen, freeze-dry and demineralised human cortical bone allograft. Cell Tissue Bank. 24 (1), 25–35. https://doi.org/10.1007/s10561-022-10013-9.

Marcos, V., Perrotti, F., Iaculli, F., Aragones, C., Benfatti, C., Magrin, G., Piattelli, G., 2019. Physical and mechanical properties of composite scaffolds with or without collagen impregnation. Appl. Sci. 9. https://doi.org/10.3390/app9204296.

Massini, C., 2022. Optimization and Validation of a Test Bench and Protocols for Characterizing the Permeability of Hard and Soft Tissue Engineering Scaffolds. Politecnico di Torino, Torino.

McKay, B., Sandhu, H.S., 2002. Use of recombinant human bone morphogenetic protein-2 in spinal fusion applications. Spine 27 (16S), 66–85.

Mellier, C., Lefèvre, F.X., Fayon, F., Montouillout, V., Despas, C., Le Ferrec, M., Boukhechba, F., Walcarius, A., Janvier, P., Dutilleul, M., Gauthier, O., Bouler, J.M., Bujoli, B., 2017. A straightforward approach to enhance the textural, mechanical and biological properties of injectable calcium phosphate apatitic cements (CPCs): CPC/blood composites, a comprehensive study. Acta Biomater. 62, 328–339. https://doi.org/10.1016/j.actbio.2017.08.040.

Melton, J.T., Wilson, A.J., Chapman-Sheath, P., Cossey, A.J., 2010a. TruFit CB bone plug: chondral repair, scaffold design, surgical technique and early experiences. Expet Rev. Med. Dev. 7 (3), 333–341. https://doi.org/10.1586/erd.10.15.

Melton, J., Bray, L., Tong, J., Cossey, A., 2010b. A biomechanical analysis of the material properties of the TruFit CB plugs for osteochondral defects of the knee. J. Bone Joint Surg. Br. 92-B (3), 420–421.

Meta Biomed Co. ltd, 2014. Silicon containing coralline hydroxyapatite bone graft substitute [Brochure]. Available from: https://www.meta-biomed.com/download/surgical/BoneMedik-S_Manual_(English).pdf.

Miller, L., Guerra, A.B., Bidros, R.S., Trahan, C., Baratta, R., Metzinger, S.E., 2005. A comparison of resistance to fracture among four commercially available forms of hydroxyapatite cement. Ann. Plast. Surg. 55 (1), 87–92. https://doi.org/10.1097/01.sap.0000162510.05196.c6.

Miller, L., Jacofsky, J., Kirker, K., Juda, Block, J., 2012. Rationale, characteristics, and clinical performance of the OsteoSponge®: a novel allograft for treatment of osseous defects. Orthop. Res. Rev. 4, 9–17. https://doi.org/10.2147/ORR.S29397.

Moon, H.S., Won, Y.Y., Kim, K.D., et al., 2004. The three-dimensional microstructure of the trabecular bone in the mandible. Surg. Radiol. Anat. 26, 466–473. https://doi.org/10.1007/s00276-004-0247-x.

Moustafa, H., Omar, S., Osman, S., Kawana, K., 2015. Effect of Collatape® collagen wound dressing alone and combined with Ingenios® synthetic bone graft on the socket healing in rabbits. Alexandria Dent. J. 40, 27–32. https://doi.org/10.21608/adjalexu.2015.58731.

Nakadate, M., Amizuka, N., Li, M., Freitas, P.H., Oda, K., Nomura, S., Uoshima, K., Maeda, T., 2008. Histological evaluation on bone regeneration of dental implant placement sites grafted with a self-setting alpha-tricalcium phosphate cement. Microsc. Res. Tech. 71 (2), 93–104. https://doi.org/10.1002/jemt.20532.

Nauth, A., Schemitsch, E., Norris, B., Nollin, Z., Watson, J.T., 2018. Critical-size bone defects: is there a consensus for diagnosis and treatment? J. Orthop. Trauma 32 (Suppl. 1), 7–11. https://doi.org/10.1097/BOT.0000000000001115.

Neen, D., Noyes, D., Shaw, M., Gwilym, S., Fairlie, N., Birch, N., 2006. Healos and bone marrow aspirate used for lumbar spine fusion: a case controlled study comparing healos with autograft. Spine 31 (18), 636–640. https://doi.org/10.1097/01.brs.0000232028.97590.12.

Nich, C., Hamadouche, M., 2011. Synthetic bone grafts: clinical use. Comprehens. Biomater. 1, 335–347. https://doi.org/10.1016/B978-0-08-055294-1.00214-2.

Niederauer, G.G., Lee, D.R., Sankaran, S., 2006. Bone grafting in arthroscopy and sports medicine. Sports Med. Arthrosc. Rev. 14 (3), 163–168. https://doi.org/10.1097/00132585-200609000-00008.

Nikodem, A., 2012. Correlations between structural and mechanical properties of human trabecular femur bone. Acta Bioeng. Biomech. 14 (2), 37–46.

Noguchi, H., Funayama, T., Koda, M., Iijima, Y., Kumagai, H., Ishikawa, T., Aiba, A., Abe, T., Nagashima, K., Miura, K., Izawa, S., Maki, S., Furuya, T., Yamazaki, M., 2019. A unidirectional porous beta-tricalcium phosphate material (Affinos®) for reconstruction of bony defects after excision of fibular bone for spinal surgery graft. J. Clin. Neurosci. 66, 71–76. https://doi.org/10.1016/j.jocn.2019.05.021.

O'Mahony, A.M., Williams, J.L., Katz, J.O., Spencer, P., 2000. Anisotropic elastic properties of cancellous bone from a human edentulous mandible. Clin. Oral Implants Res. 11 (5), 415–421. https://doi.org/10.1034/j.1600-0501.2000.011005415.x.

Ohman, C., Baleani, M., Perilli, E., Dall'Ara, E., Tassani, S., Baruffaldi, F., Viceconti, M., 2007a. Mechanical testing of cancellous bone from the femoral head: experimental errors due to off-axis measurements. J. Biomech. 40 (11), 2426–2433. https://doi.org/10.1016/j.jbiomech.2006.11.020.

Ohman, C., Baleani, M., Perilli, E., Dall'Ara, E., Tassani, S., Baruffaldi, F., Viceconti, M., 2007b. Mechanical testing of cancellous bone from the femoral head: experimental errors due to off-axis measurements. J. Biomech. 40 (11), 2426–2433. https://doi.org/10.1016/j.jbiomech.2006.11.020.

Ott, R., Wüstenhagen, C., Martin, H., Stiehm, M., Schmidt, W., Einnolf, N., Frerich, B., Grabow, N., Schmitz, K.P., Siewert, S., 2017. Experimental and numerical investigations of fluid flow for optimized in vitro stem cell loading in xenografts. Curr. Dir. Biomed. Eng. 3. https://doi.org/10.1515/cdbme-2017-0169.

Palussière, J., Berge, J., Gangi, A., Cotten, A., Pasco, A., Bertagnoli, R., Jaksche, H., Carpeggiani, P., Deramond, H., 2005. Clinical results of an open prospective study of a bis-GMA composite in percutaneous vertebral augmentation. Eur. Spine J. 14 (10), 982–991. https://doi.org/10.1007/s00586-003-0664-2.

Panseri, S., Montesi, M., Hautcoeur, D., Dozio, S.M., Chamary, S., De Barra, E., Tampieri, A., Leriche, A., 2021. Bone-like ceramic scaffolds designed with bioinspired porosity induce a different stem cell response. J. Mater. Sci. Mater. Med. 32 (1). https://doi.org/10.1007/s10856-020-06486-3.

Passuti, N., Delécrin, J., Daculsi, G., 1997. Experimental data regarding macroporous biphasic calcium phosphate ceramics. Eur. J. Orthop. Surg. Traumatol. 7, 79–84. https://doi.org/10.1007/BF00578773.

Pawelke, J., Vinayahalingam, V., Heiss, C., Budak, M., El Khassawna, T., Knapp, G., 2023. Comparison of nanocrystalline hydroxyapatite bone graft with empty defects in long bone fractures: a retrospective case-control study. Med Sci Monit 29. https://doi.org/10.12659/MSM.941112.

Pennella, F., Cerino, G., Massai, D., Gallo, D., Falvo D'Urso Labate, G., Schiavi, A., Deriu, M.A., Audenino, A., Morbiducci, U., 2013. A survey of methods for the

evaluation of tissue engineering scaffold permeability. Ann. Biomed. Eng. 41 (10), 2027–2041. https://doi.org/10.1007/s10439-013-0815-.
Perale, G., Monjo, M., Ramis, J.M., Øvrebø, Ø., Betge, F., Lyngstadaas, P., Haugen, H.J., 2019. Biomimetic biomolecules in next generation xeno-hybrid bone graft material show enhanced in vitro bone cells response. J. Clin. Med. 8. https://doi.org/10.3390/jcm8122159.
Perilli, E., Baleani, M., Ohman, C., Fognani, R., Baruffaldi, F., Viceconti, M., 2008a. Dependence of mechanical compressive strength on local variations in microarchitecture in cancellous bone of proximal human femur. J. Biomech. 41 (2), 438–446. https://doi.org/10.1016/j.jbiomech.2007.08.003.
Perilli, E., Baleani, M., Ohman, C., Fognani, R., Baruffaldi, F., Viceconti, M., 2008b. Dependence of mechanical compressive strength on local variations in microarchitecture in cancellous bone of proximal human femur. J. Biomech. 41 (2), 438–446. https://doi.org/10.1016/j.jbiomech.2007.08.003.
Perlick, L., Diedrich, O., Bäthis, H., et al., 2001. A comparison between xenogenic deproteinized bone substitute Pyrost® and autologous bone graft in the surgical management of simple bone cysts clinical and radiographic results. Eur. J. Trauma 27, 117–122. https://doi.org/10.1007/s00068-001-1079-6.
Ploumis, A., Albert, T.J., Brown, Z., Mehbod, A.A., Transfeldt, E.E., 2010. Healos graft carrier with bone marrow aspirate instead of allograft as adJct to local autograft for posterolateral fusion in degenerative lumbar scoliosis: a minimum 2-year follow-up study. J. Neurosurg. Spine 13 (2), 211–215. https://doi.org/10.3171/2010.3.SPINE09603.
Rothweiler, R., Gross, C., Bortel, E., Früh, S., Gerber, J., Boller, E., Wüster, J., Stricker, A., Fretwurst, T., Iglhaut, G., Nahles, S., Schmelzeisen, R., Hesse, B., Nelson, K., 2022. Comparison of the 3D-microstructure between alveolar and iliac bone for enhanced bioinspired bone graft substitutes. Front. Bioeng. Biotechnol. 10. https://doi.org/10.3389/fbioe.2022.862395. PMID: 35782504; PMCID: PMC9248932.
Rupprecht, S., Merten, H.A., Kessler, P., Wiltfang, J., 2003. Hydroxyapatite cement (BoneSource) for repair of critical sized calvarian defects–an experimental study. J. Cranio-Maxillo-Fac. Surg. 31 (3), 149–153. https://doi.org/10.1016/s1010-5182(03)00017-9.
Saadalla, M.E., et al., 2001. Comparison between commercial calcium phosphate bone cements. Key Eng. Mater. 218–220, 331–334. https://doi.org/10.4028/www.scientific.net/kem.218-220.331.
Saijo, H., Chung, U.I., Igawa, K., Mori, Y., Chikazu, D., Iino, M., Takato, T., 2008. Clinical application of artificial bone in the maxillofacial region. J. Artif. Organs 11 (4), 171–176. https://doi.org/10.1007/s10047-008-0425-4.
Sanus, G.Z., Tanriverdi, T., Ulu, M.O., Kafadar, A.M., Tanriover, N., Ozlen, F., 2008. Use of Cortoss as an alternative material in calvarial defects: the first clinical results in cranioplasty. J. Craniofac. Surg. 19 (1), 88–95. https://doi.org/10.1097/scs.0b013e31815c93fe.
Saragaglia, D., Blaysat, M., Inman, D., Mercier, N., 2011. Outcome of opening wedge high tibial osteotomy augmented with a Biosorb® wedge and fixed with a plate and screws in 124 patients with a mean of ten years follow-up. Int. Orthop. 35 (8), 1151–1156. https://doi.org/10.1007/s00264-010-1102-9.
Sartori, S., Silvestri, M., Forni, F., Cornaglia, A.I., Tesei, P., Cattaneo, V., 2003. Ten-year follow-up in a maxillary sinus augmentation using anorganic bovine bone (Bio-Oss). A case report with histomorphometric evaluation. Clin. Oral Implants Res. 14 (3), 369–372. https://doi.org/10.1034/j.1600-0501.2003.140316.x.
Schmidt, A.H., 2021. Autologous bone graft: is it still the gold standard? Injury 52 (Suppl. 2), 18–22.
Schröter, L., Kaiser, F., Stein, S., Gbureck, U., Ignatius, A., 2020. Biological and mechanical performance and degradation characteristics of calcium phosphate cements in large animals and humans. Acta Biomater. 117, 1–20. https://doi.org/10.1016/j.actbio.2020.09.031.
Schwarz, F., Bieling, K., Latz, T., Nuesry, E., Becker, J., 2006. Healing of intrabony peri-implantitis defects following application of a nanocrystalline hydroxyapatite (Ostim) or a bovine-derived xenograft (Bio-Oss) in combination with a collagen membrane (Bio-Gide). A case series. J. Clin. Periodontol. 33 (7), 491–499. https://doi.org/10.1111/j.1600-051X.2006.00936.x.
Seebach, C., Schultheiss, J., Wilhelm, K., Frank, J., Henrich, D., 2010. Comparison of six bone-graft substitutes regarding to cell seeding efficiency, metabolism and growth behaviour of human mesenchymal stem cells (MSC) in vitro. Injury 41 (7), 731–738. https://doi.org/10.1016/j.injury.2010.02.017.
Seto, S., Muramatsu, K., Hashimoto, T., Tominaga, Y., Taguchi, T., 2013. A new β-tricalcium phosphate with uniform triple superporous structure as a filling material after curettage of bone tumour. Anticancer Res. 33 (11), 5075–5081.
Shekhawat, D., Singh, A., Banerjee, M.K., Singh, T., Patnaik, A., 2021. Bioceramic composites for orthopaedic applications: a comprehensive review of mechanical, biological, and microstructural properties. Ceram. Int. 47 (3), 3013–3030.
Sofamor Danek, Medtronic, 2005. MASTERGRAFT® MATRIX technical guide [Brochure]. https://www.makromed.com.tr/myfiles/MASTERGRAFT20Matrix20-20Technical20Guide.pdf.
Solakoğlu, Ö., Ofluoğlu, D., Schwarzenbach, H., Heydecke, G., Reißmann, D., Ergun, S., Götz, W., 2022. A 3-year prospective randomized clinical trial of alveolar bone crest response and clinical parameters through 1, 2, and 3 years of clinical function of implants placed 4 months after alveolar ridge preservation using two different allogeneic bone-grafting materials. Int. J. Implant Dent. 8 (1). https://doi.org/10.1186/s40729-022-00402-w.
Sollazzo, V., Palmieri, A., Girardi, A., Zollino, I., Brunelli, G., Spinelli, G., Carinci, F., 2010a. Osteoplant acts on stem cells derived from peripheral blood. J. Indian Soc. Periodontol. 14 (1), 12–17. https://doi.org/10.4103/0972-124X.65429.
Sollazzo, V., Palmieri, A., Girardi, A., Farinella, F., Carinci, F., 2010b. Engipore acts on human bone marrow stem cells. Saudi Dent. J. 22 (4), 161–166. https://doi.org/10.1016/j.sdentj.2010.07.007.
Spies, C.K., Schnürer, S., Gotterbarm, T., Breusch, S., 2009. The efficacy of Biobon and Ostim within metaphyseal defects using the Göttinger Minipig. Arch. Orthop. Trauma Surg. 129 (7), 979–988. https://doi.org/10.1007/s00402-008-0705-8.
Spies, C.K., Schnürer, S., Gotterbarm, T., Breusch, S.J., 2010. Efficacy of Bone Source™ and Cementek™ in comparison with Endobon™ in critical size metaphyseal defects, using a minipig model. J. Appl. Biomater. Biomech. 8 (3), 175–185.
Steijvers, E., Ghei, A., Xia, Z., 2022. Manufacturing artificial bone allografts: a perspective. Biomater. Transl. 3 (1), 65–80. https://doi.org/10.12336/biomatertransl.2022.01.007.
Synthes® Inc, 2006a. Norian® SRS®. Trochanteric fractures in combination with DHS [Brochure]. https://www.rch.org.au/uploadedFiles/Main/Content/ortho/Norian_SRS_Trochanteric_fractures.pdf.
Synthes® Inc, 2006b. Norian® SRS®. Tibia plateau fractures [Brochure]. https://www.rch.org.au/uploadedFiles/Main/Content/ortho/Norian_SRS_Tibia_plateau_fractures.pdf.
Synthes GmbH, chronOS Inject. Synthetic bone substitute – injectable, Osteoconductive, Resorbable. [Brochure]. https://synthes.vo.llnwd.net/o16/Mobile/Synthes%20International/KYO/Trauma/PDFs/036.000.794.pdf.
Talò, G., Turrisi, C., Arrigoni, C., Recordati, C., Gerges, I., Tamplenizza, M., Cappelluti, A., Riboldi, S.A., Moretti, M., 2018. Industrialization of a perfusion bioreactor: prime example of a non-straightforward process. J. Tissue Eng. Regen. Med. 12 (2), 405–415. https://doi.org/10.1002/term.2480.
Tampieri, A., Ruffini, A., Montesi, M., Panseri, S., Salamanna, F., Fini, M., Sprio, S., 2019. Heterogeneous chemistry in the 3-D state: an original approach to generate bioactive, mechanically-competent bone scaffold. Biomater. Sci. 7, 307–321. https://doi.org/10.1039/C8BM01145A.
Teo, J.C., Si-Hoe, K.M., Keh, J.E., Teoh, S.H., 2006. Relationship between CT intensity, micro-architecture and mechanical properties of porcine vertebral cancellous bone. Clin. Biomech. 21 (3), 235–244. https://doi.org/10.1016/j.clinbiomech.2005.11.001.
Thomsen, J.S., Ebbesen, E.N., Mosekilde, L., 2002. Static histomorphometry of human iliac crest and vertebral trabecular bone: a comparative study. Bone 30 (1), 267–274. https://doi.org/10.1016/s8756-3282(01)00666-4.
Trecant, M., Delcrin, J., Roger, J., Daculsi, G., 1994. Mechanical changes in macroporous calcium phosphate ceramics after implantation in bone. Clin. Mater. 15, 233–240.
Tsuang, Y.H., Lin, F.H., Tai, H.C., Sun, J.S., Liu, H.C., Hang, Y.S., 1997. Biocompatibility and osteoconductivity of the pyrost bone substitutes. Histol. Histopathol. 12 (1), 19–24.
Urban, R.M., Turner, T.M., Hall, D.J., Infanger, S.I., Cheema, N., Lim, T.H., Moseley, J., Carroll, M., Roark, M., 2004. Effects of altered crystalline structure and increased initial compressive strength of calcium sulfate bone graft substitute pellets on new bone formation. Orthopedics 27 (Suppl. 1), 113–118. https://doi.org/10.3928/0147-7447-20040102-06.
Urrutia, J., Thumm, N., Apablaza, D., Pizarro, F., Zylberberg, A., Quezada, F., 2008. Autograft versus allograft with or without demineralized bone matrix in posterolateral lumbar fusion in rabbits. Laboratory investigation. J. Neurosurg. Spine 9 (1), 84–89. https://doi.org/10.3171/SPI/2008/9/7/084.
U.S. Food and Drug Administration OSFERION, OSFERION [510(k) no. K061499]. https://www.accessdata.fda.gov/cdrh_docs/pdf6/K061499.pdf.
U.S. Food and Drug Administration OSSATURA, OSSATURA BCP BONE VOID FILLER [510(k) no. K030131]. https://www.accessdata.fda.gov/cdrh_docs/pdf3/K030131.pdf.
US. Food and Drug Administration OSTIM, OSTIM [510(k) no. K030052]. https://www.accessdata.fda.gov/cdrh_docs/pdf3/K030052.pdf.
U.S. Food and Drug Administration POLYGRAFT, POLYGRAFT BGS; BONE GRAFT SUBSTITUTE [510(k) no. K040047]. https://www.accessdata.fda.gov/cdrh_docs/pdf4/K040047.pdf.
U.S. Food and Drug Administration VERTEBROPLASTIC, VERTEBROPLASTIC® [510(k) no. 201831]. https://www.accessdata.fda.gov/cdrh_docs/pdf20/K201831.pdf.
U.S. Food and Drug Administration, 1998a. THALAFIX NATURAL SEA SALT DRESSING [510(k) no. K980779]. Available from: https://www.accessdata.fda.gov/cdrh_docs/pdf/K980779.pdf.
U.S. Food and Drug Administration, 1998b. Pro Osteon® 500R Resorbable bone void filler. [510(k) no. K980817]. Available from: https://www.accessdata.fda.gov/cdrh_docs/pdf/K980817.pdf.
U.S. Food and Drug Administration, 2001. HEALOS BONE GRAFT MATERIAL [510(k) no. K012751]. Available from: https://www.accessdata.fda.gov/cdrh_docs/pdf/K012751.pdf.
U.S. Food and Drug Administration, 2002. CALCIGEN-S BONE VOID FILER [510(k) no. K013790]. Available from: https://www.accessdata.fda.gov/cdrh_docs/pdf/K013790.pdf.
U.S. Food and Drug Administration, 2003. BoneSource® BVF [510(k) no. K031435]. Available from: https://www.accessdata.fda.gov/cdrh_docs/pdf3/K031435.pdf.
U.S. Food and Drug Administration, 2004a. BONESAVE BONE VOID FILLER [510(k) no. K033258]. Available from: https://www.accessdata.fda.gov/cdrh_docs/pdf3/K033258.pdf.
U.S. Food and Drug Administration, 2004b. CERAFORM BONE VOID FILLER [510(k) no. K040669]. Available from: https://www.accessdata.fda.gov/cdrh_docs/pdf4/K040669.pdf.
U.S. Food and Drug Administration, 2005. IsoTis OrthoBiologics DynaGraft II [510(k) no. K040419]. Available from: https://www.accessdata.fda.gov/cdrh_docs/pdf4/K040419.pdf.
U.S. Food and Drug Administration, 2006a. HEALOS FX BONE GRAFT SUBSTITUTE AND GRAFT MIXING AND DELIVERY SYSTEM [510(k) no. K062495]. Available from: https://www.accessdata.fda.gov/cdrh_docs/pdf6/K062495.pdf.

U.S. Food and Drug Administration, 2006b. BIO 1-KIT BIOSORB filled cartridge [510(k) no. K061022]. Available from: https://www.accessdata.fda.gov/cdrh_docs/pdf6/K061022.pdf.
U.S. Food and Drug Administration, 2007a. Summary of safety and effectiveness data [510(k) no. P050053]. Available from: https://www.accessdata.fda.gov/cdrh_docs/pdf5/P050053B.pdf.
U.S. Food and Drug Administration, 2007b. BONEMEDIK, AND BONEMEDIK-S [510(k) no. K070897]. Available from: https://www.accessdata.fda.gov/cdrh_docs/pdf7/K070897.pdf.
U.S. Food and Drug Administration, 2009. ALPHA-BSM, BETA-BSM, GAMMA-BSM, EQUIVABONE [510(k) no. K091729]. Available from: https://www.accessdata.fda.gov/cdrh_docs/pdf9/K091729.pdf.
U.S. Food and Drug Administration, 2012. BICERA (TM) RESORBABLE BONE SUBSTITUTE [510(k) no. K110949]. Available from: https://www.accessdata.fda.gov/cdrh_docs/pdf11/K110949.pdf.
U.S. Food and Drug Administration, 2013. GEISTLICH BIO-OSS® [510(k) no. K12289]. Available from: https://www.accessdata.fda.gov/cdrh_docs/pdf12/K122894.pdf.
U.S. Food and Drug Administration, 2018. Straumann cerabone [510(k) no. K173594]. Available from: https://www.accessdata.fda.gov/cdrh_docs/pdf17/K173594.pdf.
U.S. Food and Drug Administration, 2019. Orthoss® [510(k) no. K190754]. Available from: https://www.accessdata.fda.gov/cdrh_docs/pdf19/K190754.pdf.
U.S. Food and Drug Administration, 2020. Cerament bone void filler [510(k) no. K201535]. Available from: https://www.accessdata.fda.gov/cdrh_docs/pdf20/K201535.pdf.
U.S. Food and Drug Administration, Stimulan KIT, STIMULAN RAPID CURE [510(k) no. K141830]. https://www.accessdata.fda.gov/cdrh_docs/pdf14/K141830.pdf.
U.S. Food and Drug Administration, CORTOSS BONE AUGMENTATION MATERIAL [510(k) no. K080108]. https://www.accessdata.fda.gov/cdrh_docs/pdf8/K080108.pdf.
U.S. Food and Drug Administration, GRAFTYS HBS [510(k) no. K082498]. https://www.accessdata.fda.gov/cdrh_docs/pdf8/K082498.pdf.
U.S. Food and Drug Administration, HydroSet XT [510(k) no. K161447]. https://www.accessdata.fda.gov/cdrh_docs/pdf16/K161447.pdf.
U.S. Food and Drug Administration, MagnetOs granules [510(k) no. K213111]. https://www.accessdata.fda.gov/cdrh_docs/pdf21/K213111.pdf.
U.S. Food and Drug Administration, MASTERGRAFT MATRIX EXT; MASTERGRAFT PUTTY, MASTERGRAFT STRIP [510(k) no. K141824]. https://www.accessdata.fda.gov/cdrh_docs/pdf14/K141824.pdf.
U.S. Food and Drug Administration, MBCP [510(k) no. K032268]. https://www.accessdata.fda.gov/cdrh_docs/pdf3/K032268.pdf.
U.S. Food and Drug Administration, MIMIX MP BONE VOID FILLER [510(k) no. K043280]. https://www.accessdata.fda.gov/cdrh_docs/pdf4/K043280.pdf.
U.S. Food and Drug Administration, NORIAN SRS BONE VOID FILLER [510(k) no. K011897]. https://www.accessdata.fda.gov/cdrh_docs/pdf/K011897.pdf.
Van der Stok, J., Van Lieshout, E.M., El-Massoudi, Y., Van Kralingen, G.H., Patka, P., 2011. Bone substitutes in The Netherlands - a systematic literature review. Acta Biomater. 7 (2), 739–750. https://doi.org/10.1016/j.actbio.2010.07.035.
van Dijk, L., Utomo, L., Yuan, H., Groot, F., Gawlitta, D., Rosenberg, A.J.W.P., de Bruijn, J., 2023a. Calcium phosphate with submicron topography influences primary human macrophage response, enhancing downstream angiogenesis and osteogenesis in vitro. J. Immunol. Regen. Med. 19. https://doi.org/10.1016/j.regen.2023.100070.
van Dijk, L.A., Janssen, N.G., Nurmohamed, S.J., Muradin, M.S.M., Longoni, A., Bakker, R.C., de Groot, F.G., de Bruijn, J.D., Gawlitta, D., Rosenberg, A.J.W.P., 2023b. Osteoinductive calcium phosphate with submicron topography as bone graft substitute for maxillary sinus floor augmentation: a translational study. Clin. Oral Implants Res. 34 (3), 177–195. https://doi.org/10.1111/clr.14028.
Van Lieshout, E.M., Van Kralingen, G.H., El-Massoudi, Y., Weinans, H., Patka, P., 2011. Microstructure and biomechanical characteristics of bone substitutes for trauma and orthopaedic surgery. BMC Muscoskel. Disord. 12. https://doi.org/10.1186/1471-2474-12-34.
Winkler, T., Sass, F.A., Duda, G.N., Schmidt-Bleek, K., 2018. A review of biomaterials in bone defect healing, remaining shortcomings and future opportunities for bone tissue engineering: the unsolved challenge. Bone Joint Res. 7 (3), 232–243. https://doi.org/10.1302/2046-3758.73.BJR-2017-0270.R1.
Wright Medical Technology, 2012. MIIG® X3 & MIIG® X3 Hivisc pastes [Brochure]. https://www.wright.com/wp-content/uploads/2015/04/129611_7_EN.pdf.
Wright Medical Technology (2021), OSTEOSET Resorbable Bead Kits [Brochure]. https://www.wrightemedia.com/ProductFiles/Files/PDFs/AP-014331_EN_LR_LE.pdf.
Wu, P.K., Chen, C.F., Chen, C.M., Tsai, S.W., Cheng, Y.C., Chang, M.C., Chen, W.M., 2018. Grafting for bone defects after curettage of benign bone tumour - analysis of factors influencing the bone healing. J. Chin. Med. Assoc. 81 (7), 643–648. https://doi.org/10.1016/j.jcma.2017.08.024.
Wu, Y., Loaiza, J., Banerji, R., Blouin, O., Morgan, E., 2021. Structure-function relationships of the human vertebral endplate. JOR Spine. 4 (3). https://doi.org/10.1002/jsp2.1170.
Yamasaki, N., Hirao, M., Nanno, K., Sugiyasu, K., Tamai, N., Hashimoto, N., Yoshikawa, H., Myoui, A., 2009. A comparative assessment of synthetic ceramic bone substitutes with different composition and microstructure in rabbit femoral condyle model. J. Biomed. Mater. Res. B Appl. Biomater. 91 (2), 788–798. https://doi.org/10.1002/jbm.b.31457.
Yao, J., Ho, A.M., 2009. Bone graft substitutes in the treatment of distal radius and upper limb injuries. Operat. Tech. Orthop. 19, 77–87.
H.Y. Yeung, L. Qin, K.M. Lee, K.S. Leung, J.C.Y. Cheng, Quantification of porosity, connectivity and material density of calcium phosphate ceramic implants using micro-computed tomography. In: L. Qin, H.K. Genant, J.F. Griffith, K.S. Leung (eds) Advanced Bioimaging Technologies in Assessment of the Quality of Bone and Scaffold Materials. Springer, Berlin, Heidelberg. doi: 10.1007/978-3-540-45456-4_17.
Yu, B., Han, K., Ma, H., Zhang, C., Su, J., Zhao, J., Li, J., Bai, Y., Tang, H., 2009. Treatment of tibial plateau fractures with high strength injectable calcium sulphate. Int. Orthop. 33 (4), 1127–1133. https://doi.org/10.1007/s00264-008-0611-2.
Zhang, X., Tiainen, H., Haugen, H.J., 2019. Comparison of titanium dioxide scaffold with commercial bone graft materials through micro-finite element modelling in flow perfusion. Med. Biol. Eng. Comput. 57 (1), 311–324. https://doi.org/10.1007/s11517-018-1884-2.
Zimmer Biomet Dental, IngeniOs® Silicated ß-TCP Synthetic Bone Particles [Brochure]. https://www.zimvie.com/content/dam/zimvie-corporate/en/dental/literature/zv1664/zv1664_ingenios_b-tcp_synthetic_bone_particles_final_secured.pdf.
Zimmer GmbH, Triosite® Bioactive Ceramic Bone Graft Substitute [Brochure]. https://www.hospitrauma.com/download/HOSPITRAUMA_ZimmerBiomet_Triosite.pdf.